

# Weak and strong deflection gravitational lensings by a charged Horndeski black hole

Cheng-Yi Wang, Yu-Fu Shen and Yi Xie<sup>1</sup>

School of Astronomy and Space Science, Nanjing University, Nanjing 210023, China  
Key Laboratory of Modern Astronomy and Astrophysics, Nanjing University, Ministry of Education, Nanjing 210023, China

E-mail: [yixie@nju.edu.cn](mailto:yixie@nju.edu.cn)

**Abstract.** A charged black hole was predicted by the Einstein–Horndeski–Maxwell theory. In order to provide its observational signatures, we investigate its weak and strong deflection gravitational lensings. We find its weak deflection lensing observables, including the positions, magnifications and differential time delay of the lensed images. We also obtain its strong deflection lensing observables, including the apparent radius of the photon sphere as well as the angular separation, brightness difference and differential time delay between the relativistic images. Taking the supermassive black hole in the Galactic Center as the lens, we evaluate these observables and compare these signatures with those of the Schwarzschild, Reissner-Nordström, tidal Reissner-Nordström and charged Galileon black holes. After a detailed analysis of the feasibility of measuring these lensing observables, we conclude that although it is possible to detect some leading effects of the weak and strong deflection lensings by the charged Horndeski and other black holes with current technology, it would be unlikely to distinguish one kind of these black holes from the others based on these detections in the near future due to lack of enough highly angular resolution in astronomical observations to tell their differences.

**Keywords:** Gravitational lensing; Modified gravity; GR black holes

---

<sup>1</sup>Corresponding author.

---

## Contents

<b>1</b>	<b>Introduction</b>	<b>1</b>
<b>2</b>	<b>Metric and gravitational lensing set-up</b>	<b>3</b>
2.1	Metric	3
2.2	Gravitational lensing set-up	4
<b>3</b>	<b>Weak deflection lensing</b>	<b>5</b>
3.1	Image positions and their relations	6
3.2	Magnifications and their relations	7
3.3	Total magnification and centroid	8
3.4	Differential time delay	9
3.5	Practical observables	11
3.6	Example for Sgr A*	12
<b>4</b>	<b>Strong deflection lensing</b>	<b>13</b>
4.1	Strong deflection limit and observables	13
4.2	Example for Sgr A*	16
<b>5</b>	<b>Conclusions and discussion</b>	<b>17</b>
<b>A</b>	<b>Weak deflection lensing by a (tidal) Reissner-Nordström black hole</b>	<b>19</b>

---

## 1 Introduction

As the most general scalar-tensor theory of gravitation in four dimensional spacetime yielding second-order field equations, the Horndeski theory was constructed in 1974 [1] by inspiration of the work of Lovelock [2]. It is recently revived again in the aftermath of severe attack from gravitational wave detection [3]. The discovery of cosmic acceleration [4, 5] has triggered an extensive search of modifications of the general relativity (GR) [6], in which the scalar-tensor theories are regarded as the most natural, simplest and consistent modification of GR and the most well studied and established alternative theories. In the last decade, the Horndeski theory has played a major role as a ghost-free effective field theory acting as dark energy because it can include GR, Brans-Dicke theory [7], the  $f(R)$  gravity [8, 9], the Dvali–Gabadadze–Porrati model [10] and the Galileon model [11–14] in some specific limits. However, after the direct detections of gravitational waves and optical counterpart of a binary neutron star merger [15–17], the extremely small difference between the phase velocity of the gravitational wave and the speed of light almost ruled out the whole Horndeski theory as a candidate of dark energy [18–23] but with few exceptions [24, 25] (see ref. [26] for a recent review). Nevertheless, it was currently found [3] that the energy scale observed at LIGO is very close to the cutoff of the Horndeski theory and the operators at the cutoff scale can bring the speed of gravitational waves to the speed of light at LIGO scale, making this theory alive again.

Astrophysics under the Horndeski theory also drew much attention. Its effects on the motions of planets and pulsars and light propagation were constrained in the Solar and stellar

systems [27–30]. While stars were obtained in this theory [31–35] and proved to be absence of scalar hair [36], Horndeski black holes [37–44] are more attractive since they might be able to evade the no-hair theorems [45–48]. Stabilities [49, 50] and thermodynamics [51, 52] of these black holes were also investigated.

As a powerful tool in gravitational physics [53], signals of both weak and strong deflection gravitational lensing carry an abundance of information on fundamental physics of black holes and nature of gravity, which might be taken to test the Horndeski theory in a different way from the gravitational waves. Weak deflection lensing has been employed to provide insights on astronomy, astrophysics and cosmology [54–58], to test GR and the modified theories of gravity [59–62] and to probe the interaction between electromagnetic and gravitational fields [63, 64]. Strong deflection lensing can generate a “shadow” and relativistic images caused by photons winding several loops around a black hole, which is a unique feature in the nearby region around the black hole and is not presented in the weak deflection lensing (see [65–67] for reviews). The photon sphere of a black hole plays an important role in the strong deflection. The Event Horizon Telescope <sup>1</sup> (EHT) is directly observing and imaging the shadows of the supermassive black hole Sgr A\* in the Galactic Center as well as the supermassive black hole at the center of M87. Strong deflection lensings by static and symmetric black holes [68–94] and rotating black holes [95–108] are widely studied and they can be used to discriminate black holes [109–114], naked singularities [115–118] and wormholes [119–123] as well as test gravity [124, 125] and its fundamental interaction with electromagnetic field [126–130]. Strong deflection lensings by a neutral Horndeski black hole [131] and by a charged Galileon black hole [112] were also studied. Nevertheless, the relativistic images of strong deflection lensing are extremely faint [73, 74, 132] and significantly hard to detect for current stage of technology. Therefore, a combination of weak and strong deflection lensing might be complementary to each other and be able to provide a whole picture of a black hole’s lensing signatures [76, 91, 133].

In this work, we will focus on the weak and strong deflection gravitational lensings by a charged Horndeski black hole. It is an asymptotically flat solution to a sub-class of the Horndeski theory with the scalar field coupled to the background only through the Einstein tensor in the presence of an electric field [39]. It is more complicated than the charged Galileon black hole considered in Ref. [112] which is a perturbative solution [40]. As we will show, their lensing signatures have some similarity in a manner but with enough difference to tell. It is widely believed that an astrophysical black hole in the real universe must have zero charge because the surrounding plasma can neutralize it. However, the electric charge of a black hole can be inherited from its charged collapsed progenitor [134], be acquired by accretion of charged matter and be induced by its rotation in the external magnetic field [135]. It was found [136] that Sgr A\* may have a small, transient positive charge.

In Sect. 2, the spacetime of the charged Horndeski black hole is briefly reviewed and the set-up for gravitational lensing is given, including its lens equation as well as its exact forms of the bending angle and travelling time span for a photon. In Sect. 3, we obtain its weak deflection lensing observables, including positions, magnifications and differential time delay of the lensed images. In Sect. 4, the strong deflection lensing observables are found out for the charged Horndeski black hole, including the apparent size of the photon sphere as well as the angular separation, brightness difference and differential time delay between the relativistic images. These results are compared with those of the Schwarzschild, Reissner-Nordström,

---

<sup>1</sup><https://eventhorizontelescope.org/>

tidal Reissner-Nordström and charged Galileon black holes in both of scenarios of lensings and their feasibility of detection are also discussed in these two sections. Finally, in Sect. 5, we summarize and discuss our results.

## 2 Metric and gravitational lensing set-up

### 2.1 Metric

In a four dimensional spacetime, the Lagrangian of the Horndeski theory has a form as [1, 38, 39]

$$L = \lambda_1 \delta_{\rho\sigma\mu\nu}^{\alpha\beta\gamma\kappa} R_{\alpha\beta}^{\rho\sigma} R_{\gamma\kappa}^{\mu\nu} + \lambda_2 \delta_{\rho\mu\nu}^{\alpha\beta\gamma} \nabla_\alpha \phi \nabla^\rho \phi R_{\beta\gamma}^{\mu\nu} + \lambda_3 \delta_{\mu\nu}^{\alpha\beta} R_{\alpha\beta}^{\mu\nu} + \Theta + B \epsilon^{\alpha\beta\gamma\kappa} R_{\nu\alpha\beta}^\mu R_{\mu\gamma\kappa}^\nu \quad (2.1)$$

where  $R_{\nu\alpha\beta}^\mu$  is the Riemann curvature tensor,  $B$  is a constant,  $\lambda_{1,2,3}$  are arbitrary functions of the scalar field  $\phi$  and  $\Theta$  is an arbitrary function of  $\nabla_\alpha \phi \nabla^\alpha \phi$  and  $\phi$ . One particular case of this theory is the scalar field couple to the background only with the Einstein tensor  $G_{\mu\nu}$  controlled by parameter  $\eta$  in the presence of an electromagnetic field  $F^{\mu\nu}$ , which reads as ( $G = c = 1$ ) [39]

$$I = \int \sqrt{-g} d^4x \left[ \frac{R}{16\pi} + \frac{\eta}{2} G_{\mu\nu} \nabla^\mu \phi \nabla^\nu \phi - \frac{1}{4} F_{\mu\nu} F^{\mu\nu} \right]. \quad (2.2)$$

It has an asymptotically flat solution describing the charged Horndeski black hole as

$$ds^2 = -A(r)dt^2 + B(r)dr^2 + C(r)(d\theta^2 + \sin^2\theta d\varphi^2) \quad (2.3)$$

with the functions  $A(r)$ ,  $B(r)$  and  $C(r)$  as

$$A(r) = 1 - \frac{2m_\bullet}{r} + \frac{Q}{r^2} - \frac{Q^2}{12r^4} \quad (2.4)$$

$$B(r) = \left(1 - \frac{Q}{2r^2}\right)^2 [A(r)]^{-1} \quad (2.5)$$

$$C(r) = r^2. \quad (2.6)$$

where  $m_\bullet$  is the mass and  $Q = q_e^2/4$  is an integration constant connected with the charge. In order to ensure the existence of the event horizon and the curvature singularities inside the horizon, the condition that [52]

$$0 < Q < \frac{9}{8}m_\bullet^2 \quad (2.7)$$

has to be satisfied.

The charged Horndeski black hole (2.3) is different from a Reissner-Nordström black hole [137, 138]

$$A_{\text{RN}}(r) = [B_{\text{RN}}(r)]^{-1} = 1 - \frac{2m_\bullet}{r} + \frac{Q}{r^2}, \quad C_{\text{RN}}(r) = r^2, \quad \text{with } 0 < Q < m_\bullet^2 \quad (2.8)$$

by an extra term of  $r^{-4}$  in  $A(r)$  and  $A(r)B(r) \neq 1$ . It was also found [52] that its thermodynamical behavior is different from the one of a Reissner-Nordström black hole by the fact that its temperature is always positive but not zero. As a solution in the braneworld

paradigm [139], the tidal Reissner-Nordström black hole [140] has the same metric as the Reissner-Nordström black hole does in the formality. The tidal charge  $Q$  controls the  $r^{-2}$  terms in both of the metrics. While  $Q$  in the Reissner-Nordström black hole is the square of its electric charge and is always positive,  $Q$  in the tidal Reissner-Nordström black hole can be negative because of the gravitational effects from the fifth dimension [140]. As a perturbative solution to the theory (2.2), the charged Galileon black hole [40] is more similar to the charged Horndeski black hole and has the metric with positive  $Q$  as

$$A_{\text{CG}}(r) = 1 - \frac{2m_{\bullet}}{r} + \frac{Q}{r^2} \quad (2.9)$$

$$B_{\text{CG}}(r) = \left(1 + \frac{Q}{r^2}\right)^{-1} [A_{\text{CG}}(r)]^{-1} \quad (2.10)$$

$$C_{\text{CG}}(r) = r^2, \quad (2.11)$$

with

$$0 < Q < m_{\bullet}^2. \quad (2.12)$$

## 2.2 Gravitational lensing set-up

Although based on quite different contexts, the mathematical descriptions of these four black hole solutions, i.e., the charged Horndeski, Reissner-Nordström, tidal Reissner-Nordström and charged Galileon black hole, are close to each other. It will be theoretically and practically interesting to know their observational signatures that might be helpful to distinguish them. In this work, we focus on their gravitational lensings, especially by a supermassive black hole, because ground-based infrared and radio interferometry [141, 142] have continuously improved capabilities to probe lensing signals of Sgr A\* and M87 and physical processes nearby them. Detection of gravitational waves from supermassive black hole binaries may have to wait for next generation space-borne detectors.

For an isolated black hole, the exact bending angle of a deflected light ray can be obtained as [73, 143]

$$\hat{\alpha}(r_0) = 2 \int_{r_0}^{\infty} \frac{\sqrt{B(r)}}{\sqrt{C(r)} \sqrt{\frac{C(r)}{C(r_0)} \frac{A(r_0)}{A(r)} - 1}} dr - \pi, \quad (2.13)$$

where  $r_0$  is the closet approach distance of the photon to the black hole. When  $r_0 \gg 2m_{\bullet}$ ,  $\hat{\alpha}$  will be much less than 1 and this integral can be handled in the small angle approximation, giving the weak deflection lensing. As  $r_0$  decreases to  $2m_{\bullet}$ ,  $\hat{\alpha}$  increases and diverges eventually, giving the strong deflection lensing. In order to find the lensing observables, we take the lens equation as [73, 74]

$$\tan \mathcal{B} = \tan \vartheta - D[\tan \vartheta + \tan(\hat{\alpha} - \vartheta)], \quad (2.14)$$

where  $\mathcal{B}$  is the angular position of the source,  $\vartheta$  is the angular position of the image,  $D = D_{\text{LS}}/D_{\text{OS}}$  and  $D_{\text{LS}}$  and  $D_{\text{OS}}$  are the angular diameter distances from the lens to the source and from the observer to the source. For a lensed image, its (signed) magnification  $\mu$  can be found as [144]

$$\mu(\vartheta) = \left[ \frac{\sin \mathcal{B}(\vartheta) d\mathcal{B}(\vartheta)}{\sin \vartheta d\vartheta} \right]^{-1}. \quad (2.15)$$

If the brightness of a source is variable, the differential time delay between its lensed images would be possibly measurable. Its value can be obtained by making use of the total time span

for a photon traveling from the source to the observer [78, 88, 143]

$$T = T(R_{\text{src}}) + T(R_{\text{obs}}), \quad (2.16)$$

with

$$T(R) = \int_{r_0}^R \left| \frac{dt}{dr} \right| dr \quad (2.17)$$

and

$$\frac{dt}{dr} = \frac{\sqrt{B(r)C(r)A(r_0)}}{A(r)\sqrt{C(r_0)}\sqrt{\frac{C(r)}{C(r_0)}\frac{A(r_0)}{A(r)} - 1}}, \quad (2.18)$$

where  $R_{\text{obs}} = D_{\text{OL}}$  is the distance from the observer to the lens and  $R_{\text{src}} = (D_{\text{OS}}^2 \tan^2 \mathcal{B} + D_{\text{LS}}^2)^{1/2}$  is the radial coordinate of the source with respect to the lens.

The bending angle, the lens equation, the magnification and the time delay will be evaluated in both weak and strong deflection lensings and their resulting observables will be discussed for a specific case of Sgr A\*.

### 3 Weak deflection lensing

In the scenario of weak deflection lensing, the closet approach distance of a light ray to the lens is much larger than its gravitational radius,  $r_0 \gg m_\bullet$ , so that no photon in the ray from the source to the observer winds around the lens. Therefore, deflection angle caused by the charged Horndeski black hole can be written in the form of a series for weak deflection lensing as

$$\hat{\alpha}(u) = 4\frac{m_\bullet}{u} + \left(\frac{15}{4} - q\right)\pi\left(\frac{m_\bullet}{u}\right)^2 + \frac{8}{3}(16 - 7q)\left(\frac{m_\bullet}{u}\right)^3 + \mathcal{O}\left(\frac{m_\bullet^4}{u^4}\right) \quad (3.1)$$

where  $u$  is the impact parameter satisfying  $C(r_0) = u^2 A(r_0)$  and  $q \equiv Q/m_\bullet^2$ .

For convenience in the following works, we define scaled variables [59–61]

$$\beta = \frac{\mathcal{B}}{\vartheta_E}, \quad \theta = \frac{\vartheta}{\vartheta_E}, \quad \hat{\tau} = \frac{\tau}{\tau_E}, \quad \varepsilon = \frac{\vartheta_\bullet}{\vartheta_E}, \quad (3.2)$$

where  $\vartheta_\bullet = \arctan(m_\bullet/D_{\text{OL}})$  is the angular gravitational radius at distance  $D_{\text{OL}}$ ,  $\tau$  is the time delay between images, the angular Einstein ring radius is

$$\vartheta_E = \sqrt{\frac{4m_\bullet D_{\text{LS}}}{D_{\text{OL}} D_{\text{OS}}}} \quad (3.3)$$

and the time scale is

$$\tau_E = 4m_\bullet. \quad (3.4)$$

We also assume the observer is far from the lens so that  $\varepsilon$  can serve as a small parameter to obtain higher-order observables for the charged Horndeski black hole. These next-to-leading-order observables will be critical for distinguishing various charged black holes by the weak deflection lensing since their leading signals are as the same as those of the Schwarzschild black hole in GR (see below for details).

After a comparison of lensing observables by the charged Horndeski, Reissner-Nordström, the tidal Reissner-Nordström and charged Galileon black holes, we find that the outcomes of the weak deflection lensings by the charged Horndeski and Galileon black holes are the same

so that specific expressions for the charged Galileon black hole are omitted. Meanwhile, the Reissner-Nordström and the tidal Reissner-Nordström black holes share the same formality but with opposite signs of the charges. Their observables of the weak deflection lensing are different from those of the charged Horndeski and Galileon black holes. However, these differences appear only in the next-to-leading-order terms. The details of weak deflection lensing by the (tidal) Reissner-Nordström black hole are given in appendix A (see also refs.[59, 145]) and they are in the forms which can be directly compared with those of the charged Horndeski and Galileon black holes.

### 3.1 Image positions and their relations

According to the small parameter  $\varepsilon$  in the weak deflection lensing, we assume that the position of a lensed image, which is a solution to the lens equation (2.14), can be expressed in the form of a series as

$$\theta = \theta_0 + \varepsilon\theta_1 + \varepsilon^2\theta_2 + \mathcal{O}(\varepsilon^3), \quad (3.5)$$

where  $\theta_0$ ,  $\theta_1$  and  $\theta_2$  are respectively its 0th-, 1st- and 2nd-order approximations. Following the well-established procedure [59–61], we substitute it into the lens equation (2.14), rearrange the lens equation in terms of  $\varepsilon$  and obtain  $\theta_n$  ( $n = 0, 1, 2$ ) by vanishing the coefficients of  $\varepsilon^n$ . We find that  $\theta_n$  for the charged Horndeski black hole are

$$\theta_0 = \frac{1}{2}(\beta + \eta), \quad (3.6)$$

$$\theta_1 = \frac{\pi}{4(\theta_0^2 + 1)} \left( \frac{15}{4} - q \right), \quad (3.7)$$

$$\begin{aligned} \theta_2 = & \frac{1}{\theta_0(\theta_0^2 + 1)^3} \left[ \frac{8}{3}D^2\theta_0^8 + D \left( \frac{64}{3}D - 16 \right) \theta_0^6 + \left( \frac{88}{3}D^2 - 32D + 16 \right) \theta_0^4 \right. \\ & \left. + \theta_0^2 \left( \frac{16}{3}D^2 - 16D + 32 - \frac{225}{128}\pi^2 \right) - \frac{16}{3}D^2 + 16 - \frac{225}{256}\pi^2 \right] \\ & - \frac{q}{\theta_0(\theta_0^2 + 1)^3} \left[ \frac{14}{3}\theta_0^4 + \left( \frac{28}{3} - \frac{15}{16}\pi^2 \right) \theta_0^2 - \frac{15}{32}\pi^2 + \frac{14}{3} \right] \\ & - \frac{q^2\pi(2\theta_0^2 + 1)}{16\theta_0(\theta_0^2 + 1)^3}, \end{aligned} \quad (3.8)$$

where  $D = D_{\text{LS}}/D_{\text{OS}}$  and

$$\eta = \sqrt{\beta^2 + 4}. \quad (3.9)$$

It is obvious that  $\theta_0$  is not affected by the charge  $q$  and its value is identical with the one of the Schwarzschild black hole in GR. The differences arise in  $\theta_1$  and  $\theta_2$  which return to the ones of the Schwarzschild black hole in the absence of  $q$  [59].

In the aforementioned equations and hereafter, we adopt the convention of refs. [59–61] that the angles of image positions are set to be positive. It means that the position of the source  $\mathcal{B}$  is positive if the image is on the same side of the lens as the source, while it is negative if the image is on the opposite side.

Therefore, we can respectively find out the positive- and negative-parity images at each orders as

$$\theta_0^\pm = \frac{1}{2}(\eta \pm |\beta|), \quad (3.10)$$

$$\theta_1^\pm = \frac{(15 - 4q)\pi}{8\eta(\eta \pm |\beta|)}, \quad (3.11)$$

$$\begin{aligned} \theta_2^\pm = & \frac{1}{\eta^3(\eta \pm |\beta|)^4} \left\{ \frac{64}{3} D^2 \beta^8 + D \left( \frac{1024}{3} D - 128 \right) \beta^6 \right. \\ & + \left( \frac{5056}{3} D^2 - 1024D + 128 \right) \beta^4 \\ & + \left( \frac{8576}{3} D^2 - 2304D + 768 - \frac{225}{16} \pi^2 \right) \beta^2 \\ & + \frac{2560}{3} D^2 - 1024D + 1024 - \frac{675}{16} \pi^2 \\ & - q \left[ \frac{112}{3} \beta^4 + \left( 224 - \frac{15}{2} \pi^2 \right) \beta^2 + \frac{896}{3} - \frac{45}{2} \pi^2 \right] \\ & \left. - q^2 \pi^2 (\beta^2 + 3) \right\} \\ & \pm \frac{\eta|\beta|}{\eta^3(\eta \pm |\beta|)^4} \left[ \frac{64}{3} D^2 \beta^6 + D \left( \frac{896}{3} D - 128 \right) \beta^4 \right. \\ & + \left( \frac{3392}{3} D^2 - 768D + 128 \right) \beta^2 \\ & + \frac{3328}{3} D^2 - 1024D + 512 - \frac{225}{16} \pi^2 \\ & \left. - q \left( \frac{112}{3} \beta^2 + \frac{448}{3} - \frac{15}{2} \pi^2 \right) - q^2 \pi^2 \right], \quad (3.12) \end{aligned}$$

which hold useful relations that

$$\theta_0^+ - \theta_0^- = |\beta|, \quad (3.13)$$

$$\theta_0^+ \theta_0^- = 1, \quad (3.14)$$

$$\theta_1^+ + \theta_1^- = \frac{15 - 4q}{16} \pi, \quad (3.15)$$

$$\theta_1^+ - \theta_1^- = -\frac{(15 - 4q)\pi|\beta|}{16\eta}, \quad (3.16)$$

$$\begin{aligned} \theta_2^+ - \theta_2^- = & -|\beta| \left[ 16 - 8D^2 - \frac{225}{256} \pi^2 \right. \\ & \left. - q \left( \frac{14}{3} - \frac{15}{32} \pi^2 \right) - \frac{1}{16} \pi^2 q^2 \right]. \quad (3.17) \end{aligned}$$

It is clearly shown again that the differences between the charged Horndeski and the Schwarzschild black hole begin to appear in the next-to-leading-order approximations.

### 3.2 Magnifications and their relations

Using the same scheme, we expand  $\mu$  into a series of  $\varepsilon$  as

$$\mu = \mu_0 + \varepsilon \mu_1 + \varepsilon^2 \mu_2 + \mathcal{O}(\varepsilon^3), \quad (3.18)$$

and obtain its 0th-, 1st- and 2nd-order approximations of the charged Horndeski black hole as

$$\mu_0 = \frac{\theta_0^4}{\theta_0^4 - 1}, \quad (3.19)$$



$$\mu_1 = -\frac{(15-4q)\pi\theta_0^3}{16(\theta_0^2+1)^3}, \quad (3.20)$$

$$\begin{aligned} \mu_2 = & \frac{\theta_0^2}{(\theta_0^2+1)^5(\theta_0^2-1)} \left[ \frac{8}{3}D^2\theta_0^8 + (48D^2 - 32D - 32)\theta_0^6 \right. \\ & + \left( \frac{272}{3}D^2 - 64D + \frac{675}{128}\pi^2 - 64 \right) \theta_0^4 \\ & \left. + (48D^2 - 32D - 32)\theta_0^2 + \frac{8}{3}D^2 \right] \\ & + \frac{q\theta_0^4}{(\theta_0^2+1)^5(\theta_0^2-1)} \left[ \frac{28}{3}\theta_0^4 + \left( \frac{56}{3} - \frac{45}{16}\pi^2 \right) \theta_0^2 + \frac{28}{3} \right] \\ & + \frac{3q^2\pi^2\theta_0^6}{8(\theta_0^2+1)^5(\theta_0^2-1)}. \end{aligned} \quad (3.21)$$

We further obtain their values for the positive- and negative-parity images as

$$\mu_0^\pm = \frac{1}{2} \pm \frac{\beta^2 + 2}{2|\beta|\eta}, \quad (3.22)$$

$$\mu_1^+ = \mu_1^- = -\frac{(15-4q)\pi}{16\eta^3}, \quad (3.23)$$

$$\begin{aligned} \mu_2^\pm = & \pm \frac{1}{|\beta|\eta^5} \left[ \frac{8}{3}D^2\beta^4 + \left( \frac{176}{3}D^2 - 32D - 32 \right) \beta^2 \right. \\ & - 128D + 192D^2 + \frac{675}{128}\pi^2 - 128 \\ & \left. + q \left( \frac{28}{3}\beta^2 + \frac{112}{3} - \frac{45}{16}\pi^2 \right) + \frac{3}{8}q^2\pi^2 \right], \end{aligned} \quad (3.24)$$

which have very simple relations

$$\mu_0^+ + \mu_0^- = 1, \quad (3.25)$$

$$\mu_1^+ - \mu_1^- = 0, \quad (3.26)$$

$$\mu_2^+ + \mu_2^- = 0. \quad (3.27)$$

and a clean combination

$$\mu_0^+\theta_1^+ + \mu_0^-\theta_1^- + \mu_1^+\theta_0^+ + \mu_1^-\theta_0^- = 0. \quad (3.28)$$

Like the situations of the image positions and their relations, the leading term of the magnifications has no difference from its corresponding value for the Schwarzschild black hole while the elegant relations of the magnifications might be potentially used in the consistency check of observations on the lensed images.

### 3.3 Total magnification and centroid

If the two lensed images cannot be practically resolved, the observables will be the total magnification of them and their magnification-weighted centroid position. With the help of eqs. (3.25)–(3.27), we can have the total magnification as

$$\mu_{\text{tot}} = |\mu^+| + |\mu^-|$$

$$= (2\mu_0^+ - 1) + 2\epsilon^2\mu_2^+ + \mathcal{O}(\epsilon^3). \quad (3.29)$$

Since  $\mu_1^+$  and  $\mu_1^-$  cancel out each other exactly due to eq. (3.26), there is no  $\mathcal{O}(\epsilon)$  term, suggesting that distinguishing the charged Horndeski black hole from the others by measuring total magnification requires the accuracy to reach the second-order level.

The magnification-weighted centroid position is defined by

$$\Theta_{\text{cent}} = \frac{\theta^+|\mu^+| - \theta^-|\mu^-|}{|\mu^+| + |\mu^-|} = \frac{\theta^+\mu^+ + \theta^-\mu^-}{\mu^+ - \mu^-}, \quad (3.30)$$

and it can be also expanded in the series of  $\epsilon$  as

$$\Theta_{\text{cent}} = \Theta_0 + \epsilon\Theta_1 + \epsilon^2\Theta_2 + \mathcal{O}(\epsilon^3), \quad (3.31)$$

where the 0th-, 1st- and 2nd-order approximations are

$$\Theta_0 = |\beta| \frac{\beta^2 + 3}{\beta^2 + 2}, \quad (3.32)$$

$$\Theta_1 = 0, \quad (3.33)$$

$$\begin{aligned} \Theta_2 = \frac{|\beta|}{\eta^2(\beta^2 + 2)} & \left[ \frac{8}{3}D^2\beta^6 + \left( \frac{104}{3}D - 16 \right) D\beta^4 + \left( \frac{272}{3}D^2 \right. \right. \\ & \left. \left. - 64D + 32 \right) \beta^2 - \frac{64}{3}D^2 - \frac{675}{128}\pi^2 + 128 \right. \\ & \left. - q \left( \frac{28}{3}\beta^2 - \frac{45}{16}\pi^2 + \frac{112}{3} \right) - \frac{3}{8}q\pi^2 \right]. \end{aligned} \quad (3.34)$$

Likewise, the  $\mathcal{O}(\epsilon)$  term in  $\Theta_{\text{cent}}$  vanishes due to the cancellation between  $\mu_1^+$  and  $\mu_1^-$ , demanding highly astrometric accuracy for any tests based on measuring the centroid position to access the second-order effects.

### 3.4 Differential time delay

The time delay is the difference between the light travel time with and without the lens and it can be expressed as [59, 60]

$$c\tau = T(R_{\text{src}}) + T(R_{\text{obs}}) - \frac{D_{\text{OS}}}{\cos \mathcal{B}}. \quad (3.35)$$

The function  $T(R)$ , see eq. (2.17), can be integrated and expanded as

$$T(R) = T_0 + \sum_{k=1}^3 \frac{m_{\bullet}^k}{r_0^k} r_0 T_k + \mathcal{O}\left(\frac{m_{\bullet}^4}{r_0^4}\right), \quad (3.36)$$

where the functions  $T_n$  in the 0th-, 1st-, 2nd- and 3rd-order approximations are

$$T_0 = \sqrt{R^2 - r_0^2}, \quad (3.37)$$

$$T_1 = \frac{\sqrt{1 - \xi^2}}{1 + \xi} + 2 \ln \left( \frac{1 + \sqrt{1 - \xi^2}}{\xi} \right), \quad (3.38)$$

$$T_2 = \left( \frac{15}{2} - 2q \right) \left( \frac{\pi}{2} - \arcsin \xi \right) - \left( 2 + \frac{5}{2}\xi \right) \frac{\sqrt{1 - \xi^2}}{(\xi + 1)^2}, \quad (3.39)$$

$$\begin{aligned}
T_3 = & -\left(\frac{15}{2} - 2q\right)\left(\frac{\pi}{2} - \arcsin \xi\right) \\
& + \frac{\sqrt{1-\xi^2}}{2(\xi+1)^2}[(35-18q)\xi^3 + (133-62q)\xi^2 \\
& + (157-70q)\xi + 60 - 26q],
\end{aligned} \tag{3.40}$$

with

$$\xi = \frac{r_0}{R}. \tag{3.41}$$

The first term  $T_0$  origins from the Euclidean geometry, while the second term is as the same as the Shapiro delay in GR which is not affected by the charged Horndeski black hole.

Changing  $r_0$  into  $u$  and using the expressions of  $R_{\text{src}}$  and  $R_{\text{obs}}$ , the scaled time delay can also be found as a series

$$\hat{\tau} = \hat{\tau}_0 + \varepsilon \hat{\tau}_1 + \mathcal{O}(\varepsilon^2), \tag{3.42}$$

where

$$\hat{\tau}_0 = \frac{1}{2} \left[ 1 + \beta^2 - \theta_0^2 - \ln \left( \frac{D_{\text{OL}} \theta_0^2 \vartheta_{\text{E}}^2}{4D_{\text{LS}}} \right) \right], \tag{3.43}$$

$$\hat{\tau}_1 = \frac{(15-4q)\pi}{16\theta_0}. \tag{3.44}$$

In principle, the  $\mathcal{O}(\varepsilon^2)$  term for  $\hat{\tau}$  could be obtained as well, but it is less significant than the  $\mathcal{O}(\varepsilon^2)$  corrections to the image positions  $\theta$  and magnifications  $\mu$ . Once again, the leading effects of the time delay cannot tell difference of the charged Horndeski black hole from the Schwarzschild black hole and detecting its next-to-leading-order term will be critical for that purpose.

However, the absolute value of the time delay for a single lensed image is never accessible in the weak deflection lensing. The practical observable is the differential time delay between the positive- and negative-parity images as

$$\Delta \hat{\tau} = \hat{\tau}_- - \hat{\tau}_+. \tag{3.45}$$

It also has a series form

$$\Delta \hat{\tau} = \Delta \hat{\tau}_0 + \varepsilon \Delta \hat{\tau}_1 + \mathcal{O}(\varepsilon^2), \tag{3.46}$$

where

$$\Delta \hat{\tau}_0 = \frac{1}{2} \eta |\beta| + \ln \left( \frac{\eta + |\beta|}{\eta - |\beta|} \right), \tag{3.47}$$

$$\Delta \hat{\tau}_1 = \frac{15-4q}{16} \pi |\beta| \tag{3.48}$$

It is theoretically feasible to test the charged Horndeski black hole by measuring the differential time delay between two lensed images but such a measurement has to reach enough accuracy beyond the differential Shapiro delay.

### 3.5 Practical observables

Using these lensing quantities and their relations, we can have practical observables for the weak deflection lensing by the charged Horndeski black hole. Therefore, the scaled variables  $(\beta, \theta, \mu, \hat{\tau})$  must be converted to the physical ones  $(\mathcal{B}, \vartheta, F, \tau)$  in which  $F$  is the flux of the light. Observables of the weak deflection lensing usually are the positions, magnitudes of brightness, centroid and differential time delay between the lensed images. The fluxes are connected to the magnifications through the flux of the source, i.e.,  $F_i = |\mu_i|F_{\text{src}}$ . Some possibly measurable observables are [59, 60]

$$P_{\text{tot}} \equiv \vartheta^+ + \vartheta^- = \mathcal{E} + \frac{15-4q}{16}\varepsilon\pi\vartheta_{\text{E}} + \mathcal{O}(\varepsilon^2), \quad (3.49)$$

$$\Delta P \equiv \vartheta^+ - \vartheta^- = |\mathcal{B}|\left(1 - \frac{15-4q}{16}\varepsilon\pi\frac{\vartheta_{\text{E}}}{\mathcal{E}}\right) + \mathcal{O}(\varepsilon^2), \quad (3.50)$$

$$F_{\text{tot}} \equiv F^+ + F^- = F_{\text{src}}\frac{\mathcal{B}^2 + 2\vartheta_{\text{E}}^2}{|\mathcal{B}|\mathcal{E}} + \mathcal{O}(\varepsilon^2), \quad (3.51)$$

$$\Delta F \equiv F^+ - F^- = F_{\text{src}} - F_{\text{src}}\frac{15-4q}{8}\varepsilon\pi\frac{\vartheta_{\text{E}}^3}{\mathcal{E}^3} + \mathcal{O}(\varepsilon^2), \quad (3.52)$$

$$S_{\text{cent}} \equiv \frac{\vartheta^+F^+ - \vartheta^-F^-}{F_{\text{tot}}} = |\mathcal{B}|\frac{\mathcal{B}^2 + 3\vartheta_{\text{E}}^2}{\mathcal{B}^2 + 2\vartheta_{\text{E}}^2} + \mathcal{O}(\varepsilon^2), \quad (3.53)$$

$$\Delta\tau = \frac{D_{\text{OL}}D_{\text{OS}}}{cD_{\text{LS}}}\left\{\frac{1}{2}|\mathcal{B}|\mathcal{E} + \vartheta_{\text{E}}^2\ln\left(\frac{\mathcal{E} + |\mathcal{B}|}{\mathcal{E} - |\mathcal{B}|}\right) + \varepsilon\frac{15-4q}{16}\pi\vartheta_{\text{E}}|\mathcal{B}| + \mathcal{O}(\varepsilon^2)\right\}, \quad (3.54)$$

where

$$\mathcal{E} = \sqrt{\mathcal{B}^2 + 4\vartheta_{\text{E}}^2}. \quad (3.55)$$

They are main signals of the weak deflection lensing by the charged Horndeski black hole. Among them, the  $\mathcal{O}(\varepsilon^2)$  terms in the practical observables are neglected because they are too small to be reachable in the foreseen future. Since the  $\mathcal{O}(\varepsilon)$  terms of the total magnification (3.29) and the centroid (3.33) are exactly cancelled, the total flux  $F_{\text{tot}}$  and the practical centroid  $S_{\text{cent}}$  of the lensed images have the  $\mathcal{O}(1)$  terms only, which are not affected by any charge  $q$ .

In order to indicate their deviations from those of the Schwarzschild black hole, we define that

$$\delta P_{\text{tot}} \equiv P_{\text{tot}} - P_{\text{tot}}(q=0) = -\frac{q}{4}\varepsilon\pi\vartheta_{\text{E}} + \mathcal{O}(\varepsilon^2), \quad (3.56)$$

$$\delta\Delta P \equiv \Delta P - \Delta P(q=0) = \frac{q}{4}\varepsilon\pi|\mathcal{B}|\frac{\vartheta_{\text{E}}}{\mathcal{E}} + \mathcal{O}(\varepsilon^2), \quad (3.57)$$

$$\delta r_{\text{tot}} \equiv 2.5\log_{10}\left[\frac{F_{\text{tot}}}{F_{\text{tot}}(q=0)}\right] = \mathcal{O}(\varepsilon^2), \quad (3.58)$$

$$\delta\Delta r \equiv 2.5\log_{10}\left[\frac{\Delta F}{\Delta F(q=0)}\right] = \frac{5}{4\ln 10}q\varepsilon\pi\frac{\vartheta_{\text{E}}^3}{\mathcal{E}^3} + \mathcal{O}(\varepsilon^2), \quad (3.59)$$

$$\delta S_{\text{cent}} \equiv S_{\text{cent}} - S_{\text{cent}}(q=0) = \mathcal{O}(\varepsilon^2), \quad (3.60)$$

$$\delta\Delta\tau \equiv \Delta\tau - \Delta\tau(q=0) = -\frac{D_{\text{OL}}D_{\text{OS}}}{4cD_{\text{LS}}}\varepsilon q\pi\vartheta_{\text{E}}|\mathcal{B}| + \mathcal{O}(\varepsilon^2), \quad (3.61)$$

where the differences between fluxes are converted into magnitudes. The deviations in  $\delta P_{\text{tot}}$ ,  $\delta\Delta P$ ,  $\delta\Delta r$  and  $\delta\Delta\tau$  are at the order of  $\varepsilon$ , making them likely to be detected in the near

future, while the deviations in  $\delta r_{\text{tot}}$  and  $\delta S_{\text{cent}}$  are smaller than them by another of order  $\varepsilon$ , rendering them hardly to be detected.

Because Sgr A\* is the only supermassive black hole with orbiting stars that can be directly observed, we consider it as the lens with  $M = 4.28 \times 10^6 M_{\odot}$  and  $D_{\text{OL}} = 8.32$  kpc [146] and a source orbiting it with a distance  $D_{\text{LS}} = 10^{-3}$  pc whose the angular Einstein radius is  $\theta_{\text{E}} = 710 \mu\text{as}$  and small parameter  $\varepsilon$  is  $7.2 \times 10^{-3}$  due to  $D_{\text{OS}} \approx D_{\text{OL}}$ . We note that the star S175 orbiting Sgr A\* has the periastron distance of  $2 \times 10^{-4}$  pc [146], less than our assumption of  $D_{\text{LS}}$ . We will discuss  $P_{\text{tot}}$ ,  $\Delta P$ ,  $\Delta F$  and  $\Delta\tau$  and their deviations from those of the Schwarzschild black hole, since  $q$  appears at their first order approximations in terms of  $\varepsilon$ .

### 3.6 Example for Sgr A\*

Figure 1 shows these lensing observables (left  $y$ -axis) and their deviations from those of the Schwarzschild black hole (right  $y$ -axis) by the charged Horndeski, Reissner-Nordström, tidal Reissner-Nordström and charged Galileon black holes with Sgr A\* as the lens for  $\beta = 0.5$ . It is worth mentioning that the charged Horndeski and the charged Galileon black holes have the same observables for the weak deflection lensing and the Reissner-Nordström and tidal Reissner-Nordström black holes have the same formulae for their weak deflection lensings and observables but with opposite signed  $q$  (see appendix A) .

For all of these black holes, the angular separations between two lensed images  $P_{\text{tot}}$  are about 1.47 milliarcsecond (mas), much larger than the current resolution of  $50 \mu\text{as}$  realized by phase referencing optical/infrared interferometry [141] so that these two images would potentially be able to resolved. For a given positive  $q$ ,  $P_{\text{tot}}$  of the Reissner-Nordström black hole is slightly bigger than the one of the charged Horndeski black hole, while the negative  $q$  makes the tidal Reissner-Nordström black hole has even larger  $P_{\text{tot}}$ . Their deviations from the one of the Schwarzschild black hole  $\delta P_{\text{tot}}$  range from  $-4$  to  $2 \mu\text{as}$ , where the deviation of the tidal Reissner-Nordström black hole is positive and the others are negative. Although the  $\delta P_{\text{tot}}$  of the charged Horndeski black hole is most significant among them, it is too small to detect for current technology. The angular differences between the two lensed images  $\Delta P$  for these black holes are all about 0.3 mas, potentially resolvable for current ability. Contrary to the cases of  $P_{\text{tot}}$ , the charged Horndeski black hole has the biggest  $\Delta P$  and the tidal Reissner-Nordström black hole has the smallest one. Their deviations from the one of the Schwarzschild black hole  $\delta\Delta P$  are mostly below the level of  $1 \mu\text{as}$ , making them undetectable for now. The normalized fluxes difference  $\Delta F/F_{\text{src}}$  for these black holes are close to 0.998 and their absolute deviations from the Schwarzschild black hole's  $\delta\Delta r$  are about  $4 \times 10^{-4}$  mag, equivalent to relative flux of about 370 parts per million (ppm), where the charged Horndeski black hole has the biggest values of these two quantities for a given  $|q|$ . Such a small difference of  $\delta\Delta r$  is (marginally) reachable for a space telescope, such as Transiting Exoplanet Survey Satellite with 300 ppm photometric resolution [147], but flares of Sgr A\* would wipe it out easily. The differential time delay between the two lensed images  $\Delta\tau$  for these black holes are at the level of 86 s and their absolute deviations from the Schwarzschild black hole's  $\delta\Delta\tau$  are less than 0.26 s. Among them, the charged Horndeski black hole has the smallest values of  $\Delta\tau$  and  $\delta\Delta\tau$  for a given  $|q|$ . These two timing signals are both significantly shorter than the time span of a typical astronomical observation session lasting for hours and, therefore, are unable to be measured.

In a summary of the weak deflection lensing by these charged black holes, we find that (1) among the lensing observables, the leading effects of  $P_{\text{tot}}$ ,  $\Delta P$  and  $\Delta F$  can be detected

by current technology; (2) among their deviations from those of the Schwarzschild black hole, only  $\delta\Delta r$  is within today's capability if the flare of Sgr A\* can be well handled; and (3) the existing technology is unable to detect the charge of these black holes and distinguish them further based on the deviations of their lensing observables from those of the Schwarzschild black hole.

## 4 Strong deflection lensing

In the scenario of strong deflection lensing, the closet approach distance of a light ray to the lens is very close to its gravitational radius so that the bending angle (2.13) will increase and eventually diverge as  $r_0$  decreases. It suggests that, before photons in the ray arrive the observer, they wind around the lens for several loops, which never happens in the weak deflection lensing.

### 4.1 Strong deflection limit and observables

An effectively analytic way to deal with such a divergence is to expand the integral of the bending angle near the photon sphere by the method of strong deflection limit [75]. The photon sphere is the innermost circular orbit for a photon and its radius satisfies the following equation [74, 148]

$$\frac{C'(r)}{C(r)} = \frac{A'(r)}{A(r)}, \quad (4.1)$$

where  $'$  denotes derivative against  $r$ . It is the biggest root of the resulting quartic equation of  $r$ , which can be found as  $r_m$ . Therefore, the deflection angle in the strong deflection lensing can be expanded as [75]

$$\hat{\alpha}(\theta) = -\bar{a} \log\left(\frac{\theta D_{OL}}{u_m} - 1\right) + \bar{b} + \mathcal{O}[(u - u_m) \log(u - u_m)], \quad (4.2)$$

where  $u$  is the impact parameter satisfying  $C(r_0) = u^2 A(r_0)$  and  $r_0$  is the closet approach distance of the photon. The subscript  $m$  means evaluating at  $r = r_m$  at the photon sphere so that  $u_m$  holds  $C(r_m) = u_m^2 A(r_m)$ . The strong deflection limit coefficients in the above equation can be obtained as [75]

$$\bar{a} = \frac{R_m}{2\sqrt{\gamma_m}}, \quad (4.3)$$

$$\bar{b} = -\pi + b_R + \bar{a} \ln\left(\frac{2\gamma_m}{A_m}\right), \quad (4.4)$$

where some immediate quantities are

$$\gamma_m = \frac{C_m(1 - A_m)^2 (A_m C_m'' - C_m A_m'')}{2A_m^2 C_m'^2}, \quad (4.5)$$

$$R_m = \frac{2(1 - A_m)\sqrt{A_m B_m}}{A_m' \sqrt{C_m}}, \quad (4.6)$$

$$b_R = \int_0^1 \left[ \frac{2(1 - A_m)\sqrt{A(z)B(z)}}{A'(z)C(z)\sqrt{\frac{A_m}{C_m} - \frac{A(z)}{C(z)}}} - \frac{R_m}{z\sqrt{\gamma_m}} \right] dz, \quad (4.7)$$

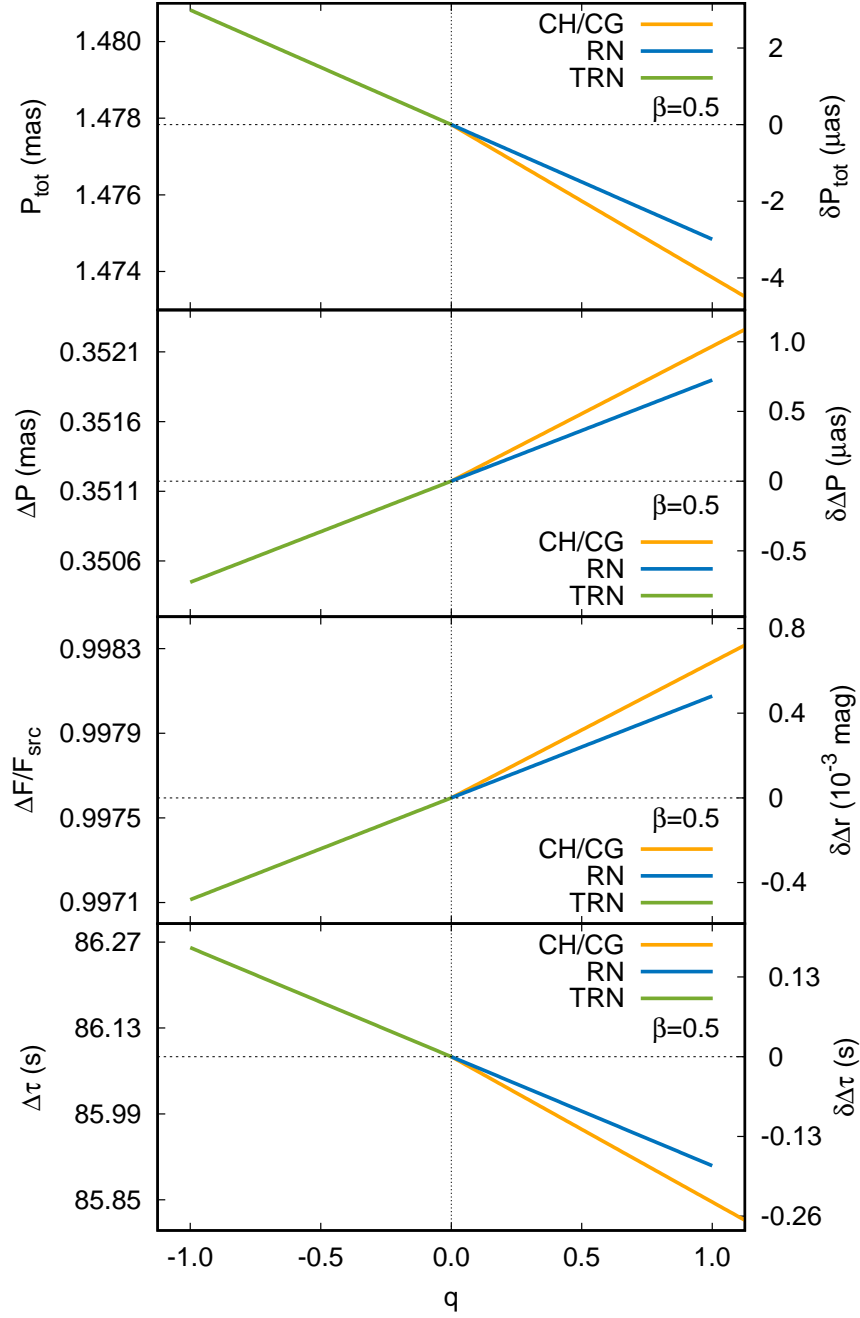


**Figure 1.** Weak deflection lensing observables (left  $y$ -axis) and their deviations from those of the Schwarzschild black hole in GR (right  $y$ -axis) by Sgr A\* in the cases of the charged Horndeski (CH), Reissner-Nordström (RN), tidal Reissner-Nordström (TRN) and charged Galileon (CG) black holes for  $\beta = 0.5$ .

and the variable  $z$  in the integral is defined by

$$z = \frac{A(r) - A_m}{1 - A_m}, \quad (4.8)$$

with ' and '' meaning derivative against  $r$  once and twice. They ensure that  $\bar{a}$  and  $\bar{b}$  can be calculated according to the metric (2.3) of the charged Horndeski black hole for any valid  $q$ . If we consider that both the source and the observer are very far from the lens and in the asymptotically flat spacetime and three of them are nearly aligned with the lens, then the lens equation (2.14) can be simplified as [72]

$$\beta = \theta - \frac{D_{\text{LS}}}{D_{\text{OS}}} [\hat{\alpha}(\theta) - 2n\pi], \quad n \in \mathbb{Z} \quad (4.9)$$

where  $\beta$ ,  $\theta$  and  $\hat{\alpha}(\theta) - 2n\pi$  are all very small. The integer  $n$  denotes the number of loops wound around by the photon, which will form the resulting relativistic image.

In order to study the differential time delay between two relativistic images of a variable source, we change the total time span, eq. (2.16), into the following form as [78]

$$T = \tilde{T}(r_0) - \int_{D_{\text{OL}}}^{\infty} \left| \frac{dt}{dr} \right| dr - \int_{D_{\text{LS}}}^{\infty} \left| \frac{dt}{dr} \right| dr. \quad (4.10)$$

Based on the facts that the source and the observer are in the asymptotically flat spacetime, we can obtain its second and third terms by means of the approach in the weak deflection lensing, while the first term coming from the strong deflection lensing is

$$\tilde{T}(r_0) = \int_{r_0}^{\infty} 2 \left| \frac{dt}{dr} \right| dr, \quad (4.11)$$

where  $dt/dr$  can be found in eq. (2.18). It can also be integrated in the strong deflection limit as [78]

$$\tilde{T}(u) = -\tilde{a} \ln \left( \frac{u}{u_m} - 1 \right) + \tilde{b} + \mathcal{O}[(u - u_m) \log(u - u_m)], \quad (4.12)$$

where  $\tilde{a}$  and  $\tilde{b}$  are strong deflection limit coefficients and  $\tilde{a} = \bar{a} u_m$  for the charged Horndeski black hole (2.3).

With the helps of the deflection angle (4.2) and the lens equation (4.9), the apparent radius of the photon sphere  $\theta_{\infty}$ , the angular separation between the first relativistic image and other packed images  $s$  and their brightness difference  $\Delta m$  can be found as [75]

$$\theta_{\infty} = \frac{u_m}{D_{\text{OL}}}, \quad (4.13)$$

$$s = \theta_{\infty} \exp \left( \frac{\bar{b}}{\bar{a}} - \frac{2\pi}{\bar{a}} \right), \quad (4.14)$$

$$\Delta m = 2.5 \log_{10} \left[ \exp \left( \frac{2\pi}{\bar{a}} \right) \right]. \quad (4.15)$$

If the brightness of the source varies, we can also calculate the differential delay between the first and second relativistic images  $\Delta T_{2,1}$  by making use of eq. (4.12) as [78]

$$\Delta T_{2,1} = \Delta T_{2,1}^0 + \Delta T_{2,1}^1, \quad (4.16)$$

where the leading and correction terms are

$$\Delta T_{2,1}^0 = 2\pi u_m, \quad (4.17)$$



$$\Delta T_{2,1}^1 = 2\sqrt{\frac{B_m}{A_m}}\sqrt{\frac{u_m}{c_m}}\exp\left(\frac{\bar{b}}{\bar{a}}\right)\left[\exp\left(-\frac{\pi}{\bar{a}}\right) - \exp\left(-\frac{2\pi}{\bar{a}}\right)\right] \quad (4.18)$$

with

$$c_m = \gamma_m\sqrt{\frac{A_m}{C_m^3}\frac{C_m'^2}{2(1-A_m)^2}} \quad (4.19)$$

and their ratio

$$\eta_{2,1} = \frac{\Delta T_{2,1}^1}{\Delta T_{2,1}}. \quad (4.20)$$

Since  $\Delta T_{2,1}^0$  is effectively equivalent to  $u_m$ , only  $\Delta T_{2,1}^1$  can provide extra information.

The effects of the charged Horndeski black hole with respect to their corresponding values of the Schwarzschild black hole in GR can also be indicated by

$$\delta\theta_\infty = \theta_\infty - \theta_\infty(q=0), \quad (4.21)$$

$$\delta s = s - s(q=0), \quad (4.22)$$

$$\delta\Delta m = \Delta m - \Delta m(q=0), \quad (4.23)$$

$$\delta\Delta T_{2,1} = \Delta T_{2,1} - \Delta T_{2,1}(q=0), \quad (4.24)$$

$$\delta\eta_{2,1} = \eta_{2,1} - \eta_{2,1}(q=0). \quad (4.25)$$

## 4.2 Example for Sgr A\*

Figure 2 shows strong deflection lensing observables (left  $y$ -axis) and their deviations from those of the Schwarzschild black hole (right  $y$ -axis) by the charged Horndeski, Reissner-Nordström, tidal Reissner-Nordström and charged Galileon black holes with Sgr A\* as the lens. The strong deflection lensing of the Reissner-Nordström, tidal Reissner-Nordström and charged Galileon black hole were respectively investigated in refs. [75, 76, 145, 149], refs. [80, 90, 109, 150, 151] and ref. [112].

For all of these black holes, their apparent radius of the photon sphere (“shadow”)  $\theta_\infty$  range from 19 to 30  $\mu\text{as}$ , which would be resolved by EHT with angular resolution of 20  $\mu\text{as}$  [142]. The negative charge  $q$  can enlarge  $\theta_\infty$  for the tidal Reissner-Nordström black hole, while the positive charge  $q$  make it shrink for the other black holes, which have almost the same curves of  $\theta_\infty$  against  $q$ . However, since the charged Horndeski black hole can have a larger  $q$  up to 9/8, it can possess an even smaller shadow. Whereas EHT can resolve the shadow, it cannot distinguish these black holes because the absolute deviations of their  $\theta_\infty$  from the one of the Schwarzschild black hole are no more than 7  $\mu\text{as}$ . The angular separations between the first relativistic image and other packed images  $s$  for these black holes change significantly from 20 to 150 nanosecond (nas). Compared with the one of the Schwarzschild black hole, the negative charge of the tidal Reissner-Nordström black hole suppress this separation, while the other black holes with positive charges can magnify it by a factor of 4 and have obviously different dependence on  $q$ . For a given positive  $q$ , the charged Horndeski black hole has the smallest values of  $s$  and its behaviour on  $s$  is more similar to the charged Galileon black hole’s than the Reissner-Nordström black hole’s. Although this situation benefits telling one kind of black hole from the others, the tininess of  $s$  makes it hardly accessible in the foreseen future. Contrary to the cases of  $s$  for these black holes, the brightness differences between the first relativistic image and other packed images  $\Delta m$  show opposite relations on  $q$ . The negative charge of the tidal Reissner-Nordström black hole can raise the contrast of them, while the positive charges of other black holes make the brightness of them closer. The magnitude of

$\Delta m$  is theoretically within the current ability of photometry but measuring it is practically impossible because there is not enough resolution to separate these relativistic images. The differential time delay between the relativistic images  $\Delta T_{2,1}$  for these black holes are all less than 14 min, where the tidal Reissner-Nordström black hole has the biggest values and others are smaller than the one of the Schwarzschild black hole by about 3 min. The curves of  $\Delta T_{2,1}$  have almost the same shapes with those of  $\theta_\infty$ , which is caused by the dominance of  $\Delta T_{2,1}^0 \propto u_m$  in  $\Delta T_{2,1}$  as the ratio of its correction to the total delay  $\eta_{2,1}$  is less than 5%.  $\Delta T_{2,1}$  of Sgr A\* is unable to measure since it is much shorter than the time span for observation sessions of EHT.

In a summary of the strong deflection lensing of these charged black holes, we find that (1) among the lensing observables, the apparent size of the photon sphere for Sgr A\* is within the current capability of EHT; (2) there is not enough resolution to distinguish these kinds of black holes based on such a measurement; and (3) resolving the relativistic images of these black holes requires technology far beyond this age so that it would be impossible to measure their angular separation, brightness difference and differential time delay in the foreseen future.

## 5 Conclusions and discussion

We investigate the weak and strong deflection gravitational lensings by the charged Horndeski black hole and compare its signals with those of the Reissner-Nordström, tidal Reissner-Nordström and charged Galileon black holes, hoping to provide hints for distinguishing these kind of black holes by observing the supermassive black hole in the Galactic Center, Sgr A\*, with infrared and radio interferometry in the future. Weak deflection lensing observables for the charged Horndeski and other black holes, including positions, magnifications and differential time delay between the lensed images and their relations are obtained. The practical observables are also constructed and analysed. We find that, for Sgr A\* as the lens, although the angular separation, angular difference and fluxes difference between the two lensed images are within the thresholds of current technology, the deviations of these observables from those of the Schwarzschild black hole are either too small to detect or easily to be wiped out by the flares of Sgr A\*. Strong deflection lensing observables, including the apparent radius of the photon sphere as well as the angular separation, brightness difference and differential time delay between the relativistic images, are found and evaluated by taking Sgr A\* as the lens. We find that only the apparent size of the photon sphere can be potentially measured by EHT whereas its resolution is not enough to distinguish these charged black holes, and there is no technology that can resolve the relativistic images of them in the foreseen future.

The charged Horndeski black hole we have discussed is a non-rotating one. Nevertheless, an astrophysical black hole is very likely spinning. This fact might make our result (partially) inapplicable if this spin is not negligible. In order to describe a rotating charged Horndeski black hole and obtain its weak and strong lensing signals, we must have its metric, which is, to our knowledge, unavailable for now. Based on previous works on light propagation and gravitational lensing by a charged and/or spinning black hole in its weak [152–168] and strong [95–98, 100, 169, 170] fields, we would expect that the spinning of an charged Horndeski black hole would shift the caustic and extend it to a finite shape, distort and displace the photon sphere, and make the lens equation more complex, which will be left for future studies. The determinations of the charge and the spacetime of Sgr A\* based on observations are also complicated works. Emissions and flares of Sgr A\* can make the lensed images in the weak

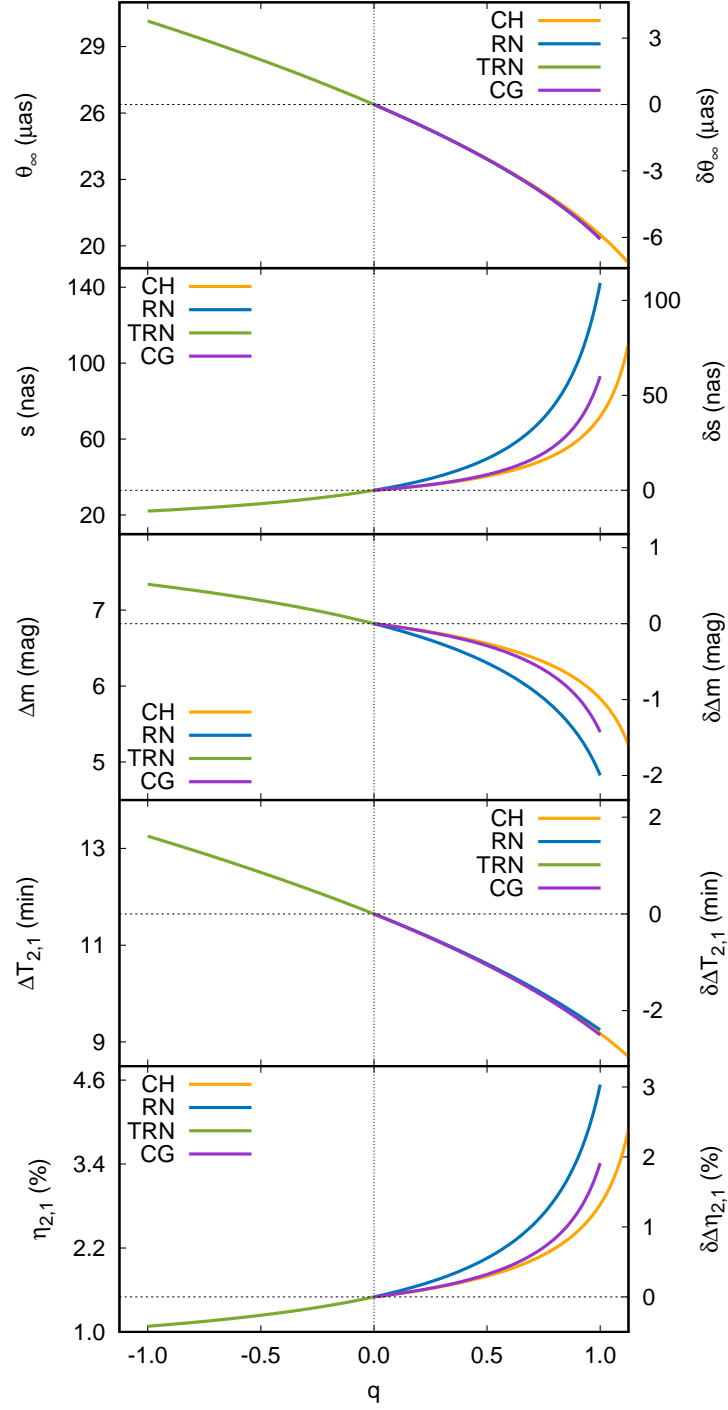


**Figure 2.** Strong deflection lensing observables (left  $y$ -axis) and their deviations from those of the Schwarzschild black hole in GR (right  $y$ -axis) by Sgr A\* in the cases of the charged Horndeski black hole (CH), Reissner-Nordström (RN), tidal Reissner-Nordström (TRN) and charged Galileon (CG) black holes.

deflection lensing hardly resolvable, while plasma in the environments of Sgr A\* and its underlying general relativistic magnetohydrodynamics can render the apparent shape of the photon sphere no longer regular. Therefore, we just give direct hints of weak and strong deflection gravitational lensing signals by a non-rotating charged Horndeski black hole with analytical methods. It indeed requires more sophisticated researches in the future.

## A Weak deflection lensing by a (tidal) Reissner-Nordström black hole

Since the Reissner-Nordström and tidal Reissner-Nordström black holes have the same metric but with opposite charge  $q$ , we only show the results of the Reissner-Nordström one here. In the weak deflection lensing, the deflection angle for a light ray caused by the Reissner-Nordström black hole is

$$\hat{\alpha}_{\text{RN}}(u) = 4\frac{m_{\bullet}}{u} + \frac{3}{4}(5-q)\pi\left(\frac{m_{\bullet}}{u}\right)^2 + 16\left(\frac{8}{3}-q\right)\left(\frac{m_{\bullet}}{u}\right)^3 + \mathcal{O}\left(\frac{m_{\bullet}^4}{u^4}\right). \quad (\text{A.1})$$

The position of its lensed image is

$$\theta_{\text{RN}} = \theta_{\text{RN}0} + \varepsilon\theta_{\text{RN}1} + \varepsilon^2\theta_{\text{RN}2} + \mathcal{O}(\varepsilon^3), \quad (\text{A.2})$$

where

$$\theta_{\text{RN}0} = \frac{1}{2}(\beta + \eta), \quad (\text{A.3})$$

$$\theta_{\text{RN}1} = \frac{3(5-q)\pi}{16(\theta_0^2 + 1)}, \quad (\text{A.4})$$

$$\begin{aligned} \theta_{\text{RN}2} = & \frac{1}{\theta_0(\theta_0^2 + 1)^3} \left[ \frac{8}{3}D^2\theta_0^8 + D\left(\frac{64}{3}D - 16\right)\theta_0^6 + \left(\frac{88}{3}D^2 - 32D + 16\right)\theta_0^4 \right. \\ & \left. + \theta_0^2\left(\frac{16}{3}D^2 - 16D + 32 - \frac{225}{128}\pi^2\right) - \frac{16}{3}D^2 + 16 - \frac{225}{256}\pi^2 \right] \\ & - \frac{q}{\theta_0(\theta_0^2 + 1)^3} \left[ 4\theta_0^4 + \left(8 - \frac{45}{64}\pi^2\right)\theta_0^2 - \frac{45}{128}\pi + 4 \right] \\ & - \frac{9q^2\pi(2\theta_0^2 + 1)}{256\theta_0(\theta_0^2 + 1)^3}. \end{aligned} \quad (\text{A.5})$$

Therefore, the positions of the positive- and negative-parity images for the Reissner-Nordström black hole are

$$\theta_{\text{RN}0}^{\pm} = \frac{1}{2}(\eta \pm |\beta|), \quad (\text{A.6})$$

$$\theta_{\text{RN}1}^{\pm} = \frac{3(5-q)\pi}{8\eta(\eta \pm |\beta|)}, \quad (\text{A.7})$$

$$\begin{aligned} \theta_{\text{RN}2}^{\pm} = & \frac{1}{\eta^3(\eta \pm |\beta|)^4} \left\{ \frac{64}{3}D^2\beta^8 + D\left(\frac{1024}{3}D - 128\right)\beta^6 \right. \\ & \left. + \left(\frac{5056}{3}D^2 - 1024D + 128\right)\beta^4 \right. \\ & \left. + \left(\frac{8576}{3}D^2 - 2304D + 768 - \frac{225}{16}\pi^2\right)\beta^2 \right\} \end{aligned}$$

$$\begin{aligned}
& + \frac{2560}{3}D^2 - 1024D + 1024 - \frac{675}{16}\pi^2 \\
& - q \left[ 32\beta^4 + \left( 192 - \frac{45}{8}\pi^2 \right) \beta^2 + 256 - \frac{135}{8}\pi^2 \right] \\
& - \frac{9}{16}q^2\pi^2(\beta^2 + 3) \Big\} \\
& \pm \frac{\eta|\beta|}{\eta^3(\eta \pm |\beta|)^4} \left[ \frac{64}{3}D^2\beta^6 + D \left( \frac{896}{3}D - 128 \right) \beta^4 \right. \\
& \left. + \left( \frac{3392}{3}D^2 - 768D + 128 \right) \beta^2 \right. \\
& \left. + \frac{3328}{3}D^2 - 1024D + 512 - \frac{225}{16}\pi^2 \right. \\
& \left. - q \left( 32\beta^2 + 128 - \frac{45}{8}\pi^2 \right) - \frac{q^2}{16}\pi^2 \right]. \tag{A.8}
\end{aligned}$$

They have relations as

$$\theta_{\text{RN}0}^+ - \theta_{\text{RN}0}^- = |\beta|, \tag{A.9}$$

$$\theta_{\text{RN}0}^+ \theta_{\text{RN}0}^- = 1, \tag{A.10}$$

$$\theta_{\text{RN}1}^+ + \theta_{\text{RN}1}^- = \frac{3(5-q)}{16}\pi, \tag{A.11}$$

$$\theta_{\text{RN}1}^+ - \theta_{\text{RN}1}^- = -\frac{3(5-q)\pi|\beta|}{16\eta}, \tag{A.12}$$

$$\begin{aligned}
\theta_{\text{RN}2}^+ - \theta_{\text{RN}2}^- = -|\beta| \left[ 16 - 8D^2 - \frac{225}{256}\pi^2 \right. \\
\left. - q \left( 4 - \frac{45}{128}\pi^2 \right) - \frac{9}{256}q^2\pi^2 \right], \tag{A.13}
\end{aligned}$$

The magnifications of the weak deflection lensing by the Reissner-Nordström black hole are

$$\mu_{\text{RN}} = \mu_{\text{RN}0} + \varepsilon\mu_{\text{RN}1} + \varepsilon^2\mu_{\text{RN}2} + \mathcal{O}(\varepsilon^3), \tag{A.14}$$

where

$$\mu_{\text{RN}0} = \frac{\theta_0^4}{\theta_0^4 - 1}, \tag{A.15}$$

$$\mu_{\text{RN}1} = -\frac{3(5-q)\pi\theta_0^3}{16(\theta_0^2 + 1)^3}, \tag{A.16}$$

$$\begin{aligned}
\mu_{\text{RN}2} = \frac{\theta_0^2}{(\theta_0^2 + 1)^5(\theta_0^2 - 1)} \left[ \frac{8}{3}D^2\theta_0^8 + (48D^2 - 32D - 32)\theta_0^6 \right. \\
\left. + \left( \frac{272}{3}D^2 - 64D + \frac{675}{128}\pi^2 - 64 \right) \theta_0^4 \right. \\
\left. + (48D^2 - 32D - 32)\theta_0^2 + \frac{8}{3}D^2 \right] \\
+ \frac{q\theta_0^4}{(\theta_0^2 + 1)^5(\theta_0^2 - 1)} \left[ 8\theta_0^4 + \left( 16 - \frac{135}{64}\pi^2 \right) \theta_0^2 + 8 \right]
\end{aligned}$$

$$+ \frac{27q^2\pi^2\theta_0^6}{128(\theta_0^2 + 1)^5(\theta_0^2 - 1)}. \quad (\text{A.17})$$

Their values for the positive- and negative-parity images are

$$\mu_{\text{RN}0}^{\pm} = \frac{1}{2} \pm \frac{\beta^2 + 2}{2|\beta|\eta}, \quad (\text{A.18})$$

$$\mu_{\text{RN}1}^+ = \mu_{\text{RN}1}^- = -\frac{3(5-q)\pi}{16\eta^3}, \quad (\text{A.19})$$

$$\begin{aligned} \mu_{\text{RN}2}^{\pm} = & \pm \frac{1}{|\beta|\eta^5} \left[ \frac{8}{3}D^2\beta^4 + \left( \frac{176}{3}D^2 - 32D - 32 \right) \beta^2 \right. \\ & - 128D + 192D^2 + \frac{675}{128}\pi^2 - 128 \\ & \left. + q \left( 8\beta^2 + 32 - \frac{135}{64}\pi^2 \right) + \frac{27}{128}q^2\pi^2 \right], \end{aligned} \quad (\text{A.20})$$

which also hold relations as

$$\mu_{\text{RN}0}^+ + \mu_{\text{RN}0}^- = 1, \quad (\text{A.21})$$

$$\mu_{\text{RN}1}^+ - \mu_{\text{RN}1}^- = 0, \quad (\text{A.22})$$

$$\mu_{\text{RN}2}^+ + \mu_{\text{RN}2}^- = 0, \quad (\text{A.23})$$

and

$$\mu_{\text{RN}0}^+\theta_{\text{RN}1}^+ + \mu_{\text{RN}0}^-\theta_{\text{RN}1}^- + \mu_{\text{RN}1}^+\theta_{\text{RN}0}^+ + \mu_{\text{RN}1}^-\theta_0^- = 0. \quad (\text{A.24})$$

The total magnification can be found as

$$\mu_{\text{RN,tot}} = (2\mu_{\text{RN}0}^+ - 1) + 2\varepsilon^2\mu_{\text{RN}2}^+ + \mathcal{O}(\varepsilon^3), \quad (\text{A.25})$$

while the position of the centroid is

$$\Theta_{\text{RN,cent}} = \Theta_{\text{RN}0} + \varepsilon\Theta_{\text{RN}1} + \varepsilon^2\Theta_{\text{RN}2} + \mathcal{O}(\varepsilon^3), \quad (\text{A.26})$$

where

$$\Theta_{\text{RN}0} = |\beta| \frac{\beta^2 + 3}{\beta^2 + 2}, \quad (\text{A.27})$$

$$\Theta_{\text{RN}1} = 0, \quad (\text{A.28})$$

$$\begin{aligned} \Theta_{\text{RN}2} = & \frac{|\beta|}{\eta^2(\beta^2 + 2)} \left[ \frac{8}{3}D^2\beta^6 + \left( \frac{104}{3}D - 16 \right) D\beta^4 + \left( \frac{272}{3}D^2 \right. \right. \\ & \left. - 64D + 32 \right) \beta^2 - \frac{64}{3}D^2 - \frac{675}{128}\pi^2 + 128 \\ & \left. - q \left( 8\beta^2 - \frac{135}{64}\pi^2 + 32 \right) - \frac{27}{128}q\pi^2 \right]. \end{aligned} \quad (\text{A.29})$$

The function  $T_{\text{RN}}(R)$  in the time delay is

$$T_{\text{RN}}(R) = T_0 + \sum_{k=1}^3 \frac{m_{\bullet}^k}{r_0^k} r_0 T_{\text{RN}k} + \mathcal{O}\left(\frac{m_{\bullet}^4}{r_0^4}\right), \quad (\text{A.30})$$

where

$$T_{\text{RN}0} = \sqrt{R^2 - r_0^2}, \quad (\text{A.31})$$

$$T_{\text{RN}1} = \frac{\sqrt{1 - \xi^2}}{1 + \xi} + 2 \ln \left( \frac{1 + \sqrt{1 - \xi^2}}{\xi} \right), \quad (\text{A.32})$$

$$T_{\text{RN}2} = \frac{3}{2}(5 - q) \left( \frac{\pi}{2} - \arcsin \xi \right) - \left( 2 + \frac{5}{2}\xi \right) \frac{\sqrt{1 - \xi^2}}{(\xi + 1)^2}, \quad (\text{A.33})$$

$$\begin{aligned} T_{\text{RN}3} = & -\frac{3}{2}(5 - q) \left( \frac{\pi}{2} - \arcsin \xi \right) \\ & + \frac{\sqrt{1 - \xi^2}}{2(\xi + 1)^2} [5(7 - 3q)\xi^3 + (133 - 52q)\xi^2 \\ & + (157 - 59q)\xi + 60 - 22q]. \end{aligned} \quad (\text{A.34})$$

It leads to the scaled time delay as

$$\hat{\tau}_{\text{RN}} = \hat{\tau}_{\text{RN}0} + \varepsilon \hat{\tau}_{\text{RN}1} + \mathcal{O}(\varepsilon^2), \quad (\text{A.35})$$

where

$$\hat{\tau}_{\text{RN}0} = \frac{1}{2} \left[ 1 + \beta^2 - \theta_0^2 - \ln \left( \frac{d_{\text{L}} \theta_0^2 \vartheta_{\text{E}}^2}{4d_{\text{LS}}} \right) \right], \quad (\text{A.36})$$

$$\hat{\tau}_{\text{RN}1} = \frac{3(5 - q)\pi}{16\theta_0}. \quad (\text{A.37})$$

Therefore, the differential time delay between the two lensed images is

$$\Delta \hat{\tau}_{\text{RN}} = \Delta \hat{\tau}_{\text{RN}0} + \varepsilon \Delta \hat{\tau}_{\text{RN}1} + \mathcal{O}(\varepsilon^2), \quad (\text{A.38})$$

where

$$\Delta \hat{\tau}_{\text{RN}0} = \frac{1}{2} \eta |\beta| + \ln \left( \frac{\eta + |\beta|}{\eta - |\beta|} \right), \quad (\text{A.39})$$

$$\Delta \hat{\tau}_{\text{RN}1} = \frac{3(5 - q)}{16} \pi |\beta| \quad (\text{A.40})$$

The practical observables for the weak deflection lensing by the Reissner-Nordström black hole are

$$P_{\text{RN,tot}} = \mathcal{E} + \frac{3(5 - q)}{16} \varepsilon \pi \vartheta_{\text{E}} + \mathcal{O}(\varepsilon^2), \quad (\text{A.41})$$

$$\Delta P_{\text{RN}} = |\mathcal{B}| \left( 1 - \frac{3(5 - q)}{16} \varepsilon \pi \frac{\vartheta_{\text{E}}}{\mathcal{E}} \right) + \mathcal{O}(\varepsilon^2), \quad (\text{A.42})$$

$$F_{\text{RN,tot}} = F_{\text{src}} \frac{\mathcal{B}^2 + 2\vartheta_{\text{E}}^2}{|\mathcal{B}| \mathcal{E}} + \mathcal{O}(\varepsilon^2), \quad (\text{A.43})$$

$$\Delta F_{\text{RN}} = F_{\text{src}} - F_{\text{src}} \frac{3(5 - q)}{8} \varepsilon \pi \frac{\vartheta_{\text{E}}^3}{\mathcal{E}^3} + \mathcal{O}(\varepsilon^2), \quad (\text{A.44})$$

$$S_{\text{RN,cent}} = |\mathcal{B}| \frac{\mathcal{B}^2 + 3\vartheta_{\text{E}}^2}{\mathcal{B}^2 + 2\vartheta_{\text{E}}^2} + \mathcal{O}(\varepsilon^2), \quad (\text{A.45})$$

$$\Delta\tau = \frac{d_L d_S}{cd_{LS}} \left\{ \frac{1}{2} |\mathcal{B}| \mathcal{E} + \vartheta_E^2 \ln \left( \frac{\mathcal{E} + |\mathcal{B}|}{\mathcal{E} - |\mathcal{B}|} \right) + \varepsilon \frac{3(5-q)}{16} \pi \vartheta_E |\mathcal{B}| + \mathcal{O}(\varepsilon^2) \right\}, \quad (\text{A.46})$$

and their deviations from those of the Schwarzschild black hole in GR are

$$\delta P_{\text{RN,tot}} = -\frac{3}{16} q \varepsilon \pi \vartheta_E + \mathcal{O}(\varepsilon^2), \quad (\text{A.47})$$

$$\delta \Delta P_{\text{RN}} = \frac{3}{16} q \varepsilon \pi |\mathcal{B}| \frac{\vartheta_E}{\mathcal{E}} + \mathcal{O}(\varepsilon^2), \quad (\text{A.48})$$

$$\delta r_{\text{RN,tot}} = \mathcal{O}(\varepsilon^2), \quad (\text{A.49})$$

$$\delta \Delta r = \frac{15}{16 \ln 10} q \varepsilon \pi \frac{\vartheta_E^3}{\mathcal{E}^3} + \mathcal{O}(\varepsilon^2), \quad (\text{A.50})$$

$$\delta S_{\text{cent}} = \mathcal{O}(\varepsilon^2), \quad (\text{A.51})$$

$$\delta \Delta \tau = -\frac{3d_L d_S}{16cd_{LS}} \varepsilon q \pi \vartheta_E |\mathcal{B}| + \mathcal{O}(\varepsilon^2). \quad (\text{A.52})$$

The tidal Reissner-Nordström black hole shares the same formulae in this appendix but with a negative  $q$ .

## Acknowledgments

This work is funded by the National Natural Science Foundation of China (Grant Nos. 11573015 and 11833004).

## References

- [1] G. W. Horndeski, *Second-Order Scalar-Tensor Field Equations in a Four-Dimensional Space*, *Int. J. Theor. Phys.* **10** (1974) 363.
- [2] D. Lovelock, *The Einstein Tensor and Its Generalizations*, *J. Math. Phys.* **12** (1971) 498.
- [3] C. de Rham and S. Melville, *Gravitational Rainbows: LIGO and Dark Energy at its Cutoff*, *Phys. Rev. Lett.* **121** (2018) 221101 [[1806.09417](#)].
- [4] A. G. Riess, A. V. Filippenko, P. Challis, A. Clocchiatti, A. Diercks, P. M. Garnavich et al., *Observational Evidence from Supernovae for an Accelerating Universe and a Cosmological Constant*, *Astron. J.* **116** (1998) 1009.
- [5] SUPERNOVA COSMOLOGY PROJECT collaboration, *Measurements of Omega and Lambda from 42 High-Redshift Supernovae*, *Astrophys. J.* **517** (1999) 565.
- [6] T. Clifton, P. G. Ferreira, A. Padilla and C. Skordis, *Modified gravity and cosmology*, *Phys. Rep.* **513** (2012) 1.
- [7] C. Brans and R. H. Dicke, *Mach's Principle and a Relativistic Theory of Gravitation*, *Phys. Rev.* **124** (1961) 925.
- [8] A. De Felice and S. Tsujikawa, *f(R) Theories*, *Living Rev. Relativ.* **13** (2010) 3 [[1002.4928](#)].
- [9] T. P. Sotiriou and V. Faraoni, *f(R) theories of gravity*, *Rev. Mod. Phys.* **82** (2010) 451 [[0805.1726](#)].
- [10] G. Dvali, G. Gabadadze and M. Porrati, *4D gravity on a brane in 5D Minkowski space*, *Phys. Lett. B* **485** (2000) 208 [[hep-th/0005016](#)].
- [11] C. Deffayet, G. Esposito-Farèse and A. Vikman, *Covariant Galileon*, *Phys. Rev. D* **79** (2009) 084003 [[0901.1314](#)].



- [12] C. Deffayet, S. Deser and G. Esposito-Farèse, *Generalized Galileons: All scalar models whose curved background extensions maintain second-order field equations and stress tensors*, *Phys. Rev. D* **80** (2009) 064015 [0906.1967].
- [13] T. Kobayashi, M. Yamaguchi and J. Yokoyama, *Generalized G-Inflation – Inflation with the Most General Second-Order Field Equations*, *Progr. Theor. Phys.* **126** (2011) 511 [1105.5723].
- [14] C. Deffayet and D. A. Steer, *A formal introduction to Horndeski and Galileon theories and their generalizations*, *Class. Quantum Gravity* **30** (2013) 214006 [1307.2450].
- [15] B. P. Abbott, R. Abbott, T. D. Abbott, F. Acernese, K. Ackley, C. Adams et al., *GW170817: Observation of Gravitational Waves from a Binary Neutron Star Inspiral*, *Phys. Rev. Lett.* **119** (2017) 161101 [1710.05832].
- [16] B. P. Abbott, R. Abbott, T. D. Abbott, F. Acernese, K. Ackley, C. Adams et al., *Multi-messenger Observations of a Binary Neutron Star Merger*, *Astrophys. J. Lett.* **848** (2017) L12 [1710.05833].
- [17] B. P. Abbott, R. Abbott, T. D. Abbott, F. Acernese, K. Ackley, C. Adams et al., *Gravitational Waves and Gamma-Rays from a Binary Neutron Star Merger: GW170817 and GRB 170817A*, *Astrophys. J. Lett.* **848** (2017) L13 [1710.05834].
- [18] L. Lombriser and N. A. Lima, *Challenges to self-acceleration in modified gravity from gravitational waves and large-scale structure*, *Phys. Lett. B* **765** (2017) 382 [1602.07670].
- [19] L. Lombriser and A. Taylor, *Breaking a dark degeneracy with gravitational waves*, *JCAP* **03** (2016) 031 [1509.08458].
- [20] T. Baker, E. Bellini, P. G. Ferreira, M. Lagos, J. Noller and I. Sawicki, *Strong Constraints on Cosmological Gravity from GW170817 and GRB 170817A*, *Phys. Rev. Lett.* **119** (2017) 251301 [1710.06394].
- [21] P. Creminelli and F. Vernizzi, *Dark Energy after GW170817 and GRB170817A*, *Phys. Rev. Lett.* **119** (2017) 251302 [1710.05877].
- [22] J. Sakstein and B. Jain, *Implications of the Neutron Star Merger GW170817 for Cosmological Scalar-Tensor Theories*, *Phys. Rev. Lett.* **119** (2017) 251303 [1710.05893].
- [23] J. M. Ezquiaga and M. Zumalacárregui, *Dark Energy After GW170817: Dead Ends and the Road Ahead*, *Phys. Rev. Lett.* **119** (2017) 251304 [1710.05901].
- [24] A. Casalino, M. Rinaldi, L. Sebastiani and S. Vagnozzi, *Mimicking dark matter and dark energy in a mimetic model compatible with GW170817*, *Phys. Dark Univ.* **22** (2018) 108 [1803.02620].
- [25] A. Casalino, M. Rinaldi, L. Sebastiani and S. Vagnozzi, *Alive and well: mimetic gravity and a higher-order extension in light of GW170817*, *Class. Quantum Gravity* **36** (2019) 017001 [1811.06830].
- [26] M. Ishak, *Testing general relativity in cosmology*, *Living Rev. Relativ.* **22** (2019) 1 [1806.10122].
- [27] M. Hohmann, *Parametrized post-Newtonian limit of Horndeski’s gravity theory*, *Phys. Rev. D* **92** (2015) 064019 [1506.04253].
- [28] S. Bhattacharya and S. Chakraborty, *Constraining some Horndeski gravity theories*, *Phys. Rev. D* **95** (2017) 044037 [1607.03693].
- [29] S. Hou and Y. Gong, *Constraints on Horndeski theory using the observations of Nordtvedt effect, Shapiro time delay and binary pulsars*, *Eur. Phys. J. C* **78** (2018) 247 [1711.05034].
- [30] P. I. Dyadina, N. A. Avdeev and S. O. Alexeyev, *Horndeski gravity without screening in binary pulsars*, *Mon. Not. R. Astron. Soc.* **483** (2019) 947 [1811.05393].

- [31] A. Cisterna, T. Delsate and M. Rinaldi, *Neutron stars in general second order scalar-tensor theory: The case of nonminimal derivative coupling*, *Phys. Rev. D* **92** (2015) 044050 [1504.05189].
- [32] A. Cisterna, T. Delsate, L. Ducobu and M. Rinaldi, *Slowly rotating neutron stars in the nonminimal derivative coupling sector of Horndeski gravity*, *Phys. Rev. D* **93** (2016) 084046 [1602.06939].
- [33] E. Babichev, C. Charmousis and A. Lehébel, *Black holes and stars in Horndeski theory*, *Class. Quantum Gravity* **33** (2016) 154002 [1604.06402].
- [34] A. Maselli, H. O. Silva, M. Minamitsuji and E. Berti, *Neutron stars in Horndeski gravity*, *Phys. Rev. D* **93** (2016) 124056 [1603.04876].
- [35] H. O. Silva, A. Maselli, M. Minamitsuji and E. Berti, *Compact objects in Horndeski gravity*, *Int. J. Mod. Phys. D* **25** (2016) 1641006 [1602.05997].
- [36] A. Lehébel, E. Babichev and C. Charmousis, *A no-hair theorem for stars in Horndeski theories*, *JCAP* **07** (2017) 037 [1706.04989].
- [37] M. Rinaldi, *Black holes with nonminimal derivative coupling*, *Phys. Rev. D* **86** (2012) 084048 [1208.0103].
- [38] A. Anabalón, A. Cisterna and J. Oliva, *Asymptotically locally AdS and flat black holes in Horndeski theory*, *Phys. Rev. D* **89** (2014) 084050 [1312.3597].
- [39] A. Cisterna and C. Erices, *Asymptotically locally AdS and flat black holes in the presence of an electric field in the Horndeski scenario*, *Phys. Rev. D* **89** (2014) 084038 [1401.4479].
- [40] E. Babichev, C. Charmousis and M. Hassaine, *Charged Galileon black holes*, *JCAP* **05** (2015) 31 [1503.02545].
- [41] E. Babichev, C. Charmousis, A. Lehébel and T. Moskalaets, *Black holes in a cubic Galileon universe*, *JCAP* **09** (2016) 011 [1605.07438].
- [42] E. Babichev, C. Charmousis and A. Lehébel, *Asymptotically flat black holes in Horndeski theory and beyond*, *JCAP* **04** (2017) 027 [1702.01938].
- [43] G. Antoniou, A. Bakopoulos and P. Kanti, *Black-hole solutions with scalar hair in Einstein-scalar-Gauss-Bonnet theories*, *Phys. Rev. D* **97** (2018) 084037 [1711.07431].
- [44] A. Bakopoulos, G. Antoniou and P. Kanti, *Novel black-hole solutions in einstein-scalar-gauss-bonnet theories with a cosmological constant*, *Phys. Rev. D* **99** (2019) 064003.
- [45] L. Hui and A. Nicolis, *No-Hair Theorem for the Galileon*, *Phys. Rev. Lett.* **110** (2013) 241104 [1202.1296].
- [46] T. P. Sotiriou and S.-Y. Zhou, *Black Hole Hair in Generalized Scalar-Tensor Gravity*, *Phys. Rev. Lett.* **112** (2014) 251102 [1312.3622].
- [47] T. P. Sotiriou and S.-Y. Zhou, *Black hole hair in generalized scalar-tensor gravity: An explicit example*, *Phys. Rev. D* **90** (2014) 124063 [1408.1698].
- [48] G. Antoniou, A. Bakopoulos and P. Kanti, *Evasion of No-Hair Theorems and Novel Black-Hole Solutions in Gauss-Bonnet Theories*, *Phys. Rev. Lett.* **120** (2018) 131102 [1711.03390].
- [49] A. Anabalón, J. Bičák and J. Saavedra, *Hairy black holes: Stability under odd-parity perturbations and existence of slowly rotating solutions*, *Phys. Rev. D* **90** (2014) 124055 [1405.7893].
- [50] A. Cisterna, M. Cruz, T. Delsate and J. Saavedra, *Nonminimal derivative coupling scalar-tensor theories: Odd-parity perturbations and black hole stability*, *Phys. Rev. D* **92** (2015) 104018 [1508.06413].

- [51] Y.-G. Miao and Z.-M. Xu, *Thermodynamics of Horndeski black holes with non-minimal derivative coupling*, *Eur. Phys. J. C* **76** (2016) 638 [[1607.06629](#)].
- [52] X.-H. Feng, H.-S. Liu, H. Lü and C. N. Pope, *Thermodynamics of charged black holes in Einstein-Horndeski-Maxwell theory*, *Phys. Rev. D* **93** (2016) 044030 [[1512.02659](#)].
- [53] V. Perlick, *Gravitational Lensing from a Spacetime Perspective*, *Living Rev. Relativ.* **7** (2004) 9.
- [54] P. Schneider, J. Ehlers and E. E. Falco, *Gravitational Lenses*. Springer-Verlag, Berlin, 1992, [10.1007/978-3-662-03758-4](#).
- [55] A. O. Petters, H. Levine and J. Wambsganss, *Singularity Theory and Gravitational Lensing*. Birkhäuser, Boston, 2001, [10.1007/978-1-4612-0145-8](#).
- [56] P. Schneider, C. S. Kochanek and J. Wambsganss, *Gravitational Lensing: Strong, Weak and Micro*, in *Saas-Fee Advanced Course 33: Gravitational Lensing: Strong, Weak and Micro*, G. Meylan, P. Jetzer and P. North, eds., (Berlin), Springer-Verlag, 2006, [DOI](#).
- [57] E. Aubourg, P. Barette, S. Bréhin, M. Gros, M. Lachièze-Rey, B. Laurent et al., *Evidence for gravitational microlensing by dark objects in the Galactic halo*, *Nature* **365** (1993) 623.
- [58] K. C. Sahu, J. Anderson, S. Casertano, H. E. Bond, P. Bergeron, E. P. Nelan et al., *Relativistic deflection of background starlight measures the mass of a nearby white dwarf star*, *Science* **356** (2017) 1046 [[1706.02037](#)].
- [59] C. R. Keeton and A. O. Petters, *Formalism for testing theories of gravity using lensing by compact objects: Static, spherically symmetric case*, *Phys. Rev. D* **72** (2005) 104006 [[gr-qc/0511019](#)].
- [60] C. R. Keeton and A. O. Petters, *Formalism for testing theories of gravity using lensing by compact objects. II. Probing post-post-Newtonian metrics*, *Phys. Rev. D* **73** (2006) 044024 [[gr-qc/0601053](#)].
- [61] C. R. Keeton and A. O. Petters, *Formalism for testing theories of gravity using lensing by compact objects. III. Braneworld gravity*, *Phys. Rev. D* **73** (2006) 104032 [[gr-qc/0603061](#)].
- [62] T. E. Collett, L. J. Oldham, R. J. Smith, M. W. Auger, K. B. Westfall, D. Bacon et al., *A precise extragalactic test of General Relativity*, *Science* **360** (2018) 1342 [[1806.08300](#)].
- [63] G. Li and X.-M. Deng, *Classical tests of photons coupled to Weyl tensor in the Solar System*, *Ann. Phys.* **382** (2017) 136.
- [64] W.-G. Cao and Y. Xie, *Weak deflection gravitational lensing for photons coupled to Weyl tensor in a Schwarzschild black hole*, *Eur. Phys. J. C* **78** (2018) 191.
- [65] V. Bozza, *Gravitational lensing by black holes*, *Gen. Relativ. Gravit.* **42** (2010) 2269 [[0911.2187](#)].
- [66] E. F. Eiroa, *Strong deflection gravitational lensing*, *arXiv:1212.4535* (2012) [[1212.4535](#)].
- [67] P. V. P. Cunha and C. A. R. Herdeiro, *Shadows and strong gravitational lensing: a brief review*, *Gen. Relativ. Gravit.* **50** (2018) 42 [[1801.00860](#)].
- [68] C. Darwin, *The Gravity Field of a Particle*, *Proc. R. Soc. Lond. Ser. A* **249** (1959) 180.
- [69] J.-P. Luminet, *Image of a spherical black hole with thin accretion disk*, *Astron. Astrophys.* **75** (1979) 228.
- [70] H. C. Ohanian, *The black hole as a gravitational “lens”*, *Am. J. Phys.* **55** (1987) 428.
- [71] R. J. Nemiroff, *Visual distortions near a neutron star and black hole*, *Am. J. Phys.* **61** (1993) 619 [[astro-ph/9312003](#)].
- [72] V. Bozza, S. Capozziello, G. Iovane and G. Scarpetta, *Strong Field Limit of Black Hole Gravitational Lensing*, *Gen. Relativ. Gravit.* **33** (2001) 1535 [[gr-qc/0102068](#)].

- [73] K. S. Virbhadra, D. Narasimha and S. M. Chitre, *Role of the scalar field in gravitational lensing*, *Astron. Astrophys.* **337** (1998) 1 [[astro-ph/9801174](#)].
- [74] K. S. Virbhadra and G. F. R. Ellis, *Schwarzschild black hole lensing*, *Phys. Rev. D* **62** (2000) 084003 [[astro-ph/9904193](#)].
- [75] V. Bozza, *Gravitational lensing in the strong field limit*, *Phys. Rev. D* **66** (2002) 103001 [[gr-qc/0208075](#)].
- [76] E. F. Eiroa, G. E. Romero and D. F. Torres, *Reissner-Nordström black hole lensing*, *Phys. Rev. D* **66** (2002) 024010 [[gr-qc/0203049](#)].
- [77] A. Bhadra, *Gravitational lensing by a charged black hole of string theory*, *Phys. Rev. D* **67** (2003) 103009 [[gr-qc/0306016](#)].
- [78] V. Bozza and L. Mancini, *Time Delay in Black Hole Gravitational Lensing as a Distance Estimator*, *Gen. Relativ. Gravit.* **36** (2004) 435 [[gr-qc/0305007](#)].
- [79] V. Perlick, *Exact gravitational lens equation in spherically symmetric and static spacetimes*, *Phys. Rev. D* **69** (2004) 064017 [[gr-qc/0307072](#)].
- [80] R. Whisker, *Strong gravitational lensing by braneworld black holes*, *Phys. Rev. D* **71** (2005) 064004 [[astro-ph/0411786](#)].
- [81] A. S. Majumdar and N. Mukherjee, *Braneworld Black Holes in Cosmology and Astrophysics*, *Int. J. Mod. Phys. D* **14** (2005) 1095 [[astro-ph/0503473](#)].
- [82] E. F. Eiroa and D. F. Torres, *Strong field limit analysis of gravitational retrolensing*, *Phys. Rev. D* **69** (2004) 063004 [[gr-qc/0311013](#)].
- [83] E. F. Eiroa, *Braneworld black hole gravitational lens: Strong field limit analysis*, *Phys. Rev. D* **71** (2005) 083010 [[gr-qc/0410128](#)].
- [84] E. F. Eiroa, *Gravitational lensing by Einstein-Born-Infeld black holes*, *Phys. Rev. D* **73** (2006) 043002 [[gr-qc/0511065](#)].
- [85] S. V. Iyer and A. O. Petters, *Light's bending angle due to black holes: from the photon sphere to infinity*, *Gen. Relativ. Gravit.* **39** (2007) 1563 [[gr-qc/0611086](#)].
- [86] N. Mukherjee and A. S. Majumdar, *Particle motion and gravitational lensing in the metric of a dilaton black hole in a de Sitter universe*, *Gen. Relativ. Gravit.* **39** (2007) 583 [[astro-ph/0605224](#)].
- [87] V. Bozza, *Comparison of approximate gravitational lens equations and a proposal for an improved new one*, *Phys. Rev. D* **78** (2008) 103005 [[0807.3872](#)].
- [88] K. S. Virbhadra and C. R. Keeton, *Time delay and magnification centroid due to gravitational lensing by black holes and naked singularities*, *Phys. Rev. D* **77** (2008) 124014 [[0710.2333](#)].
- [89] K. S. Virbhadra, *Relativistic images of Schwarzschild black hole lensing*, *Phys. Rev. D* **79** (2009) 083004 [[0810.2109](#)].
- [90] A. Y. Bin-Nun, *Gravitational lensing of stars orbiting Sgr A\* as a probe of the black hole metric in the Galactic center*, *Phys. Rev. D* **82** (2010) 064009 [[1004.0379](#)].
- [91] E. F. Eiroa and C. M. Sendra, *Gravitational lensing by massless braneworld black holes*, *Phys. Rev. D* **86** (2012) 083009 [[1207.5502](#)].
- [92] E. F. Eiroa and C. M. Sendra, *Regular phantom black hole gravitational lensing*, *Phys. Rev. D* **88** (2013) 103007 [[1308.5959](#)].
- [93] S.-S. Zhao and Y. Xie, *Strong deflection gravitational lensing by a modified Hayward black hole*, *Eur. Phys. J. C* **77** (2017) 272 [[1704.02434](#)].
- [94] S.-S. Zhao and Y. Xie, *Strong deflection lensing by a Lee-Wick black hole*, *Phys. Lett. B* **774** (2017) 357.

- [95] V. Bozza, *Quasiequatorial gravitational lensing by spinning black holes in the strong field limit*, *Phys. Rev. D* **67** (2003) 103006 [[gr-qc/0210109](#)].
- [96] S. E. Vázquez and E. P. Esteban, *Strong-field gravitational lensing by a Kerr black hole*, *Nuovo Cimento B Ser.* **119** (2004) 489 [[gr-qc/0308023](#)].
- [97] V. Bozza, F. de Luca, G. Scarpetta and M. Sereno, *Analytic Kerr black hole lensing for equatorial observers in the strong deflection limit*, *Phys. Rev. D* **72** (2005) 083003 [[gr-qc/0507137](#)].
- [98] V. Bozza, F. de Luca and G. Scarpetta, *Kerr black hole lensing for generic observers in the strong deflection limit*, *Phys. Rev. D* **74** (2006) 063001 [[gr-qc/0604093](#)].
- [99] V. Bozza and G. Scarpetta, *Strong deflection limit of black hole gravitational lensing with arbitrary source distances*, *Phys. Rev. D* **76** (2007) 083008 [[0705.0246](#)].
- [100] V. Bozza, *Optical caustics of Kerr spacetime: The full structure*, *Phys. Rev. D* **78** (2008) 063014 [[0806.4102](#)].
- [101] S. Chen and J. Jing, *Geodesic precession and strong gravitational lensing in dynamical Chern-Simons-modified gravity*, *Class. Quantum Gravity* **27** (2010) 225006 [[1005.1325](#)].
- [102] S. Chen, Y. Liu and J. Jing, *Strong gravitational lensing in a squashed Kaluza-Klein Gödel black hole*, *Phys. Rev. D* **83** (2011) 124019 [[1102.0086](#)].
- [103] G. V. Kraniotis, *Precise analytic treatment of Kerr and Kerr-(anti) de Sitter black holes as gravitational lenses*, *Class. Quantum Gravity* **28** (2011) 085021 [[1009.5189](#)].
- [104] S. Chen and J. Jing, *Strong gravitational lensing by a rotating non-Kerr compact object*, *Phys. Rev. D* **85** (2012) 124029 [[1204.2468](#)].
- [105] G. V. Kraniotis, *Gravitational lensing and frame dragging of light in the Kerr-Newman and the Kerr-Newman (anti) de Sitter black hole spacetimes*, *Gen. Relativ. Gravit.* **46** (2014) 1818 [[1401.7118](#)].
- [106] L. Ji, S. Chen and J. Jing, *Strong gravitational lensing in a rotating Kaluza-Klein black hole with squashed horizons*, *J. High Energy Phys.* **3** (2014) 89 [[1312.4128](#)].
- [107] P. V. P. Cunha, C. A. R. Herdeiro, E. Radu and H. F. Rúnarsson, *Shadows of Kerr Black Holes with Scalar Hair*, *Phys. Rev. Lett.* **115** (2015) 211102 [[1509.00021](#)].
- [108] S. Wang, S. Chen and J. Jing, *Strong gravitational lensing by a Konoplya-Zhidenko rotating non-Kerr compact object*, *JCAP* **11** (2016) 020 [[1609.00802](#)].
- [109] A. Y. Bin-Nun, *Relativistic images in Randall-Sundrum II braneworld lensing*, *Phys. Rev. D* **81** (2010) 123011 [[0912.2081](#)].
- [110] G. N. Gyulchev and S. S. Yazadjiev, *Kerr-Sen dilaton-axion black hole lensing in the strong deflection limit*, *Phys. Rev. D* **75** (2007) 023006 [[gr-qc/0611110](#)].
- [111] G. N. Gyulchev and I. Z. Stefanov, *Gravitational lensing by phantom black holes*, *Phys. Rev. D* **87** (2013) 063005 [[1211.3458](#)].
- [112] S.-S. Zhao and Y. Xie, *Strong field gravitational lensing by a charged Galileon black hole*, *JCAP* **07** (2016) 007 [[1603.00637](#)].
- [113] R. T. Cavalcanti, A. Goncalves da Silva and R. da Rocha, *Strong deflection limit lensing effects in the minimal geometric deformation and Casadio-Fabbri-Mazzacurati solutions*, *Class. Quantum Gravity* **33** (2016) 215007 [[1605.01271](#)].
- [114] S. Chakraborty and S. SenGupta, *Strong gravitational lensing—a probe for extra dimensions and Kalb-Ramond field*, *JCAP* **7** (2017) 045 [[1611.06936](#)].
- [115] G. N. Gyulchev and S. S. Yazadjiev, *Gravitational lensing by rotating naked singularities*, *Phys. Rev. D* **78** (2008) 083004 [[0806.3289](#)].

- [116] S. Sahu, M. Patil, D. Narasimha and P. S. Joshi, *Can strong gravitational lensing distinguish naked singularities from black holes?*, *Phys. Rev. D* **86** (2012) 063010 [[1206.3077](#)].
- [117] S. Sahu, M. Patil, D. Narasimha and P. S. Joshi, *Time delay between relativistic images as a probe of cosmic censorship*, *Phys. Rev. D* **88** (2013) 103002 [[1310.5350](#)].
- [118] K. S. Virbhadra and G. F. Ellis, *Gravitational lensing by naked singularities*, *Phys. Rev. D* **65** (2002) 103004.
- [119] P. K. F. Kuhfittig, *Gravitational lensing of wormholes in the galactic halo region*, *Eur. Phys. J. C* **74** (2014) 2818 [[1311.2274](#)].
- [120] P. K. F. Kuhfittig, *Gravitational lensing of wormholes in noncommutative geometry*, *arXiv:1501.06085* (2015) [[1501.06085](#)].
- [121] K. K. Nandi, Y.-Z. Zhang and A. V. Zakharov, *Gravitational lensing by wormholes*, *Phys. Rev. D* **74** (2006) 024020 [[gr-qc/0602062](#)].
- [122] N. Tsukamoto, T. Harada and K. Yajima, *Can we distinguish between black holes and wormholes by their Einstein-ring systems?*, *Phys. Rev. D* **86** (2012) 104062 [[1207.0047](#)].
- [123] N. Tsukamoto, *Strong deflection limit analysis and gravitational lensing of an ellis wormhole*, *Phys. Rev. D* **94** (2016) 124001.
- [124] E. F. Eiroa and C. M. Sendra, *Strong deflection lensing by charged black holes in scalar-tensor gravity*, *Eur. Phys. J. C* **74** (2014) 3171 [[1408.3390](#)].
- [125] H. Sotani and U. Miyamoto, *Strong gravitational lensing by an electrically charged black hole in eddington-inspired born-infeld gravity*, *Phys. Rev. D* **92** (2015) 044052.
- [126] S. Chen and J. Jing, *Strong gravitational lensing for the photons coupled to Weyl tensor in a Schwarzschild black hole spacetime*, *JCAP* **10** (2015) 002 [[1502.01088](#)].
- [127] X. Lu, F.-W. Yang and Y. Xie, *Strong gravitational field time delay for photons coupled to Weyl tensor in a Schwarzschild black hole*, *Eur. Phys. J. C* **76** (2016) 357 [[1606.02932](#)].
- [128] S. Chen, S. Wang, Y. Huang, J. Jing and S. Wang, *Strong gravitational lensing for the photons coupled to a Weyl tensor in a Kerr black hole spacetime*, *Phys. Rev. D* **95** (2017) 104017 [[1611.08783](#)].
- [129] R. Zhang and J. Jing, *Strong gravitational lensing for photons coupled to Weyl tensor in a regular phantom black hole*, *Eur. Phys. J. C* **78** (2018) 796.
- [130] S. Chen, L. Zhang and J. Jing, *A new asymptotical flat and spherically symmetric solution in the generalized Einstein-Cartan-Kibble-Sciama gravity and gravitational lensing*, *Eur. Phys. J. C* **78** (2018) 981 [[1804.05004](#)].
- [131] J. Badía and E. F. Eiroa, *Gravitational lensing by a Horndeski black hole*, *Eur. Phys. J. C* **77** (2017) 779 [[1707.02970](#)].
- [132] A. O. Petters, *On relativistic corrections to microlensing effects: applications to the Galactic black hole*, *Mon. Not. R. Astron. Soc.* **338** (2003) 457 [[astro-ph/0208500](#)].
- [133] Z. Horváth, L. Á. Gergely, Z. Keresztes, T. Harko and F. S. N. Lobo, *Constraining Hořava-Lifshitz gravity by weak and strong gravitational lensing*, *Phys. Rev. D* **84** (2011) 083006 [[1105.0765](#)].
- [134] S. Ray, A. L. Espíndola, M. Malheiro, J. P. Lemos and V. T. Zanchin, *Electrically charged compact stars and formation of charged black holes*, *Phys. Rev. D* **68** (2003) 084004 [[astro-ph/0307262](#)].
- [135] R. M. Wald, *Black hole in a uniform magnetic field*, *Phys. Rev. D* **10** (1974) 1680.
- [136] M. Zajaček, A. Tursunov, A. Eckart and S. Britzen, *On the charge of the Galactic centre black hole*, *Mon. Not. R. Astron. Soc.* **480** (2018) 4408 [[1808.07327](#)].

- [137] H. Reissner, *Über die Eigengravitation des elektrischen Feldes nach der Einsteinschen Theorie*, *Annalen der Physik* **355** (1916) 106.
- [138] G. Nordström, *On the Energy of the Gravitation field in Einstein's Theory*, *Koninklijke Nederlandse Akademie van Wetenschappen* **20** (1918) 1238.
- [139] R. Maartens, *Brane-World Gravity*, *Living Reviews in Relativity* **7** (2004) 7 [[gr-qc/0312059](#)].
- [140] N. Dadhich, R. Maartens, P. Papadopoulos and V. Rezania, *Black holes on the brane*, *Physics Letters B* **487** (2000) 1 [[hep-th/0003061](#)].
- [141] GRAVITY Collaboration, *First light for GRAVITY: Phase referencing optical interferometry for the Very Large Telescope Interferometer*, *Astron. Astrophys.* **602** (2017) A94 [[1705.02345](#)].
- [142] S. S. Doeleman, J. Weintroub, A. E. E. Rogers, R. Plambeck, R. Freund, R. P. J. Tilanus et al., *Event-horizon-scale structure in the supermassive black hole candidate at the Galactic Centre*, *Nature* **455** (2008) 78 [[0809.2442](#)].
- [143] S. Weinberg, *Gravitation and Cosmology: Principles and Applications of the General Theory of Relativity*. Wiley, New York, July, 1972.
- [144] S. Refsdal, *The gravitational lens effect*, *Mon. Not. R. Astron. Soc.* **128** (1964) 295.
- [145] X. Pang and J. Jia, *Gravitational lensing of massive particles in Reissner-Nordström black hole spacetime*, *Class. Quantum Gravity* **36** (2019) 065012.
- [146] S. Gillessen, P. M. Plewa, F. Eisenhauer, R. Sari and et al., *An Update on Monitoring Stellar Orbits in the Galactic Center*, *Astrophys. J.* **837** (2017) 30.
- [147] C. X. Huang, J. Burt, A. Vanderburg, M. N. Günther, A. Shporer, J. A. Dittmann et al., *TESS Discovery of a Transiting Super-Earth in the  $\pi$  Mensae System*, *Astrophys. J. Lett.* **868** (2018) L39 [[1809.05967](#)].
- [148] C.-M. Claudel, K. S. Virbhadra and G. F. R. Ellis, *The geometry of photon surfaces*, *J. Math. Phys.* **42** (2001) 818 [[gr-qc/0005050](#)].
- [149] A. F. Zakharov, F. de Paolis, G. Ingrosso and A. A. Nucita, *Direct measurements of black hole charge with future astrometrical missions*, *Astron. Astrophys.* **442** (2005) 795.
- [150] Z. Horváth and L. Á. Gergely, *Black hole tidal charge constrained by strong gravitational lensing*, *Astron. Nachr.* **334** (2013) 1047 [[1203.6576](#)].
- [151] A. F. Zakharov, *Constraints on a charge in the Reissner-Nordström metric for the black hole at the Galactic Center*, *Phys. Rev. D* **90** (2014) 062007.
- [152] J. Ibanez, *Gravitational lenses with angular momentum*, *Astron. Astrophys.* **124** (1983) 175.
- [153] I. Bray, *Kerr black hole as a gravitational lens*, *Phys. Rev. D* **34** (1986) 367.
- [154] S. A. Klioner, *Influence of the Quadrupole Field and Rotation of Objects on Light Propagation*, *Sov. Astron.* **35** (1991) 523.
- [155] J. F. Glicenstein, *Gravitational lensing by rotating stars*, *Astron. Astrophys.* **343** (1999) 1025.
- [156] M. Sereno and F. de Luca, *Analytical Kerr black hole lensing in the weak deflection limit*, *Phys. Rev. D* **74** (2006) 123009 [[astro-ph/0609435](#)].
- [157] M. C. Werner and A. O. Petters, *Magnification relations for Kerr lensing and testing cosmic censorship*, *Phys. Rev. D* **76** (2007) 064024 [[0706.0132](#)].
- [158] M. Sereno and F. de Luca, *Primary caustics and critical points behind a Kerr black hole*, *Phys. Rev. D* **78** (2008) 023008 [[0710.5923](#)].
- [159] A. B. Aazami, C. R. Keeton and A. O. Petters, *Lensing by Kerr black holes. I. General lens equation and magnification formula*, *J. Math. Phys.* **52** (2011) 092502 [[1102.4300](#)].

- [160] A. B. Aazami, C. R. Keeton and A. O. Petters, *Lensing by Kerr black holes. II: Analytical study of quasi-equatorial lensing observables*, *J. Math. Phys.* **52** (2011) 102501 [[1102.4304](#)].
- [161] G. He and W. Lin, *Roto-Translational Effects on Deflection of Light and Particle by Moving Kerr Black Hole*, *Int. J. Mod. Phys. D* **23** (2014) 1450031.
- [162] G. He, C. Jiang and W. Lin, *Second post-Minkowskian metric for a moving Kerr black hole*, *Int. J. Mod. Phys. D* **23** (2014) 1450079.
- [163] X.-M. Deng, *The second post-Newtonian light propagation and its astrometric measurement in the solar system*, *Int. J. Mod. Phys. D* **24** (2015) 1550056 [[1504.04084](#)].
- [164] G.-S. He and W.-B. Lin, *Second post-Minkowskian order harmonic metric for a moving Kerr-Newman black hole*, *Res. Astron. Astrophys.* **15** (2015) 646.
- [165] X.-M. Deng, *The second post-Newtonian light propagation and its astrometric measurement in the Solar System: Light time and frequency shift*, *Int. J. Mod. Phys. D* **25** (2016) 1650082.
- [166] G. He and W. Lin, *Second order Kerr-Newman time delay*, *Phys. Rev. D* **93** (2016) 023005.
- [167] G. He and W. Lin, *Second-order time delay by a radially moving Kerr-Newman black hole*, *Phys. Rev. D* **94** (2016) 063011.
- [168] G. He and W. Lin, *Analytical derivation of second-order deflection in the equatorial plane of a radially moving Kerr-Newman black hole*, *Class. Quantum Gravity* **34** (2017) 105006.
- [169] J. M. Bardeen, *Timelike and null geodesics in the Kerr metric.*, in *Black Holes (Les Astres Occlus)*, C. Dewitt and B. S. Dewitt, eds., pp. 215–239, Gordon and Breach, 1973.
- [170] S. V. Iyer and E. C. Hansen, *Light's bending angle in the equatorial plane of a Kerr black hole*, *Phys. Rev. D* **80** (2009) 124023 [[0907.5352](#)].